© 2014. Published by The Company of Biologists Ltd | Development (2014) 141, 1260-1271 doi:10.1242/dev.102327

RESEARCH ARTICLE

Dbx1 triggers crucial molecular programs required for midline crossing by midbrain commissural axons

Yasuyuki Inamata and Ryuichi Shirasaki*

ABSTRACT

Axon guidance by commissural neurons has been well documented, providing us with a molecular logic of how midline crossing is achieved during development. Despite these advances, knowledge of the intrinsic genetic programs is still limited and it remains obscure whether the expression of a single transcription factor is sufficient to activate transcriptional programs that ultimately enable midline crossing. Here, we show in the mouse that the homeodomain transcription factor Dbx1 is expressed by a subset of progenitor cells that give rise to commissural neurons in the dorsal midbrain. Gain- and loss-of-function analyses indicate that the expression of Dbx1 alone is sufficient and necessary to trigger midline crossing *in vivo*. We also show that Robo3 controls midline crossing as a crucial downstream effector of the Dbx1-activated molecular programs. Furthermore, Dbx1 suppresses the expression of the transcriptional program for ipsilateral neuron differentiation in parallel. These results suggest that a single transcription factor, Dbx1, has an essential function in assigning midline-crossing identity, thereby contributing crucially to the establishment of the wiring laterality in the developing nervous system.

KEY WORDS: Dbx1, Transcriptional program, Commissural neurons, Axon guidance, Midline crossing, Robo3, Mouse

INTRODUCTION

In the developing nervous system, navigating axons have to 'decide' whether or not to cross the midline in order to project to their specific cellular targets. The establishment of axonal projection laterality is a fundamental step for the construction of the proper neural circuits. In general, axon guidance depends upon the ability of individual axons to recognize specific guidance cues (Tessier-Lavigne and Goodman, 1996). Accumulating evidence now suggests that the intrinsic genetic programs for sensing these guidance cues are in most cases encoded by unique transcription factors that ultimately induce the expression of specific guidance receptors and receptor-associated co-factors (Shirasaki and Pfaff, 2002; Polleux et al., 2007). However, knowledge of the intrinsic genetic programs that specify the laterality of axonal projections is still limited. Importantly, for example, it remains obscure whether the expression of a single transcription factor is sufficient to trigger downstream transcriptional cascades required for midline crossing, or whether the parallel actions of several transcription factors are required to determine axonal projection laterality.

In the developing retina, the zinc finger transcription factor Zic2 is a determinant for the ipsilateral guidance programs of retinal ganglion cells (RGCs) at the ventrotemporal (VT) area (Herrera et al., 2003). Indeed, the expression of guidance receptor EphB1 is triggered by Zic2 in uncrossed RGCs, which therefore contributes to these axons' avoidance of the midline by the repulsive action of ephrin B2 expressed at around the optic chiasm (García-Frigola et al., 2008; Lee et al., 2008). It has also been reported through the analysis of *Isl2* knockout mice that the LIM homeodomain (LIM-HD) transcription factor Isl2 is involved in the assignment of the midline-crossing guidance program to crossed RGCs (Pak et al., 2004). It should be noted, however, that Isl2-mediated Zic2 repression seems to be restricted to the VT area (Pak et al., 2004). Thus, it is uncertain whether the expression of Isl2 alone is sufficient to confer axon guidance programs for midline crossing.

In the developing dorsal spinal cord, the basic helix-loop-helix (bHLH) transcription factor Atoh1 is crucially involved in the generation of dI1-type commissural neurons (Helms and Johnson, 1998; Bermingham et al., 2001; Gowan et al., 2001; Wilson et al., 2008). This suggested a possibility that Atoh1 acts as a dedicated factor that specifically triggers commissural neuron differentiation. However, it seems unlikely, as recent results have indicated that Atoh1 is also required for the generation of ipsilateral neurons (Wilson et al., 2008). Within the Atoh1 transcriptional cascade, both commissural and ipsilateral neurons postmitotically express two closely related LIM-HD transcription factors, Lhx2 and Lhx9 (Wilson et al., 2008). Interestingly, the analysis of the *Lhx2* and *Lhx9* double-knockout mice has indicated that these factors regulate the expression of Robo3 (Wilson et al., 2008), which is an essential regulator for midline crossing (Marillat et al., 2004; Sabatier et al., 2004; Tamada et al., 2008) by selectively silencing the repellent action of Slit-Robo1 signaling (Sabatier et al., 2004). Although this gene-targeting study suggests that these LIM-HD factors are required for midline crossing by commissural axons, it is currently obscure whether the expression of these factors is sufficient to specify axonal projection laterality. In addition, the mammalian Bar-class transcription factor Barhl2, which is expressed in both commissural and ipsilateral neurons of Atoh1-derived lineage, has recently been shown to be involved preferentially in the assignment of ipsilateral neuron identity (Ding et al., 2012). Therefore, it remains unclear whether there is a certain transcription factor assigned genetically, in a dedicated manner, to the acquisition of axon guidance programs required for midline crossing.

In this study, we have addressed the issue of whether a single transcription factor has an ability to trigger downstream transcriptional cascades required for midline crossing *in vivo*. For this, we employed gain- and loss-of-function strategies using an *in vivo* electroporation technique developed for mouse embryos (Tabata and Nakajima, 2001; Saito, 2006; Shimogori and Ogawa, 2008). We examined development of commissural neurons in the midbrain for the current purpose because of the following advantages. First, the size of the midbrain neural tube is the largest compared with that of the other axial levels, such as the spinal cord.

Cellular and Molecular Neurobiology Laboratory, Graduate School of Frontier Biosciences, Osaka University, Suita, Osaka 565-0871, Japan.

*Author for correspondence (shirasaki@fbs.osaka-u.ac.jp)

Received 8 August 2013; Accepted 13 January 2014

Development (2014) doi:10.1242/dev.102327

This enabled us to perform precise and reproducible *in vivo* electroporation at early stages of the mouse embryo. Second, because the axonal trajectory of commissural and ipsilateral neurons in the midbrain is anatomically and evolutionarily well documented as tectospinal and tectobulbar tracts, respectively (Murray and Coulter, 1982; Kröger and Schwarz, 1990; Shepherd and Taylor, 1995; Mastick and Easter, 1996; Shirasaki et al., 1996), the contrasting phenotype (i.e. to cross or not to cross) after gene manipulation is easily distinguishable. Here, we show that a single progenitor homeodomain factor Dbx1, expressed by a subset of progenitor cells in the dorsal midbrain, has an essential role in assigning midline-crossing identity by activating the downstream molecular programs that ultimately control the expression of Robo3 in commissural neurons.

RESULTS

Axonal trajectory of commissural neurons in the mouse midbrain

In the developing midbrain, both commissural (i.e. tectospinal) and ipsilateral (i.e. tectobulbar) neurons are generated from the same dorsal area (Murray and Coulter, 1982; Kröger and Schwarz, 1990; Shepherd and Taylor, 1995; Mastick and Easter, 1996). It has previously been shown in mice that the long projection neurons in the dorsal midbrain are generated at around embryonic day 10 (E10) (Mastick and Easter, 1996). We therefore first examined the development of midbrain commissural axons in mice by introducing green fluorescent protein (GFP)-expression vector using *in vivo* electroporation at E10.75. Three days after the electroporation, embryos were taken out and flat-mounted to analyze the entire trajectories of GFP-labeled axons (Fig. 1A). As expected, we found that commissural as well as ipsilateral axons were labeled by GFP (Fig. 1B,B′). After commissural axons had crossed the floor plate, these axons made a sharp turn to project caudally in the region between the floor plate and the oculomotor neurons, as revealed by GFP-labeled axonal trajectory together with immunostaining for expression of ALCAM, the molecular marker for motoneurons and floor plate cells (Weiner et al., 2004) (supplementary material Fig. S1A-C′). This observation is consistent with the previously reported DiI-labeling of tectofugal tracts in the mouse and chick midbrain (Shepherd and Taylor, 1995; Mastick and Easter, 1996). By contrast, when we performed electroporation at E11.5, the majority of GFP-labeled axons were ipsilateral, with few commissural axons labeled (Fig. 1C,C′,D). Here we took advantage of this experimental condition (i.e. the developmental stage used for *in vivo* electroporation), in order to examine the genetic program that directs the differentiation of midbrain commissural neurons in the mouse.

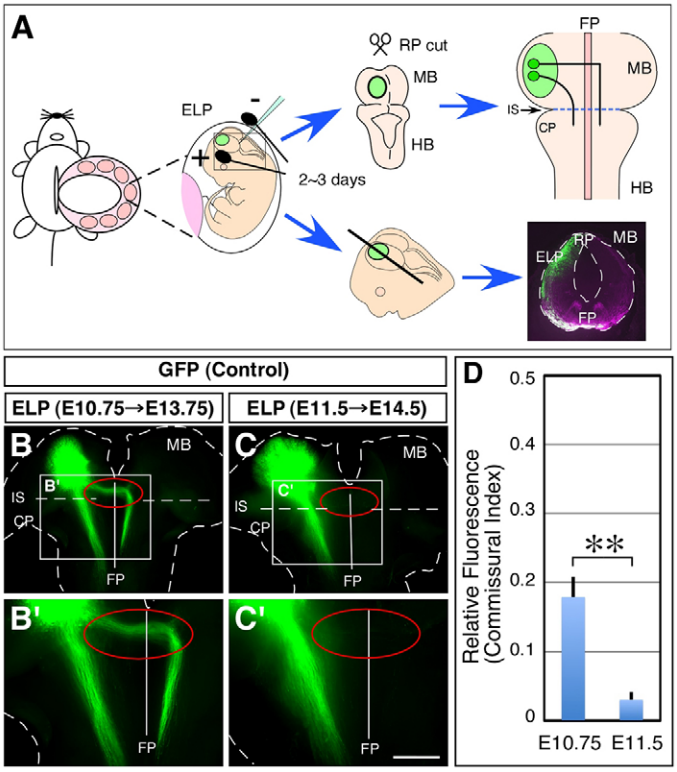

Fig. 1. Development of midbrain commissural axons revealed by mouse *in vivo* electroporation. (A) Schematic showing an outline of experimental procedures for the analysis of midbrain commissural neuron development in mice. *In vivo* electroporation was performed in the dorsal midbrain at E10.75 or E11.5. Two to 3 days after electroporation, the electroporated embryos were taken out from the mother. The neural tube containing the midbrain and hindbrain regions was cut along the roof plate, and flat-mounted to analyze the entire trajectory of GFP-labeled axons. Electroporated midbrains were also analyzed in transverse cryosections. Areas colored green denote the electroporated regions. (B-C′) Trajectory of GFP-labeled axons observed in flat-mounted midbrain/hindbrain preparations. The embryos were electroporated at E10.75 (B,B′; *n*=8) and E11.5 (C,C′; *n*=10), respectively. (B′,C′) Higher magnification views of white boxes in B,C, respectively. The red oval denotes the ventral midbrain tegmentum, which includes the floor plate, where midbrain commissural axons extend. (D) Quantification of midline crossing assessed by commissural index (see Materials and Methods). Commissural neurons can be transfected more efficiently when electroporated at E10.75 compared with E11.5 electroporation (**P<0.01, Mann-Whitney U-test). Error bars indicate s.e.m. Scale bar: 920 µm in B,C; 460 µm in B′,C′. CP, cerebellar plate; ELP, electroporation; FP, floor plate; HB, hindbrain; IS, isthmus; MB, midbrain; RP, roof plate.

Molecular characterization of midbrain commissural neurons

We have previously shown that commissural neurons in the dorsal neural tube, from the spinal cord rostrally to the midbrain where floor plate cells are found, share axon guidance mechanisms at least in the context of Netrin-mediated chemoattraction signaling (Shirasaki et al., 1995; Shirasaki et al., 1996). Here, we further characterized the expression of cell surface molecules that may be involved in the guidance of midbrain commissural axons. We first examined Robo3 expression using whole-mount immunohistochemistry on flat-mounted midbrain preparations, as Robo3 has been shown to be a crucial regulator for midline crossing by commissural axons in the spinal cord and the hindbrain (Marillat et al., 2004; Sabatier et al., 2004; Tamada et al., 2008). We found that Robo3 was selectively expressed on axons growing toward the floor plate, as judged by expression analysis of the pan-neuronal marker Tuj1 and Robo3 (Fig. 2A-C″). In addition, Robo1 was found to be expressed on the pre-crossing segment of these Robo3-expressing commissural axons (Fig. 2D-F″), as well as on the post-crossing portion of these axons at high levels (supplementary material Fig. S1D-F′). Furthermore, Robo1 was also expressed on Robo3-negative ipsilateral axons (Fig. 2D-F″; supplementary material Fig. S2).

We next analyzed the expression of transcription factors in the dorsal midbrain that have previously been shown to be expressed by commissural neurons in the dorsal spinal cord (Liem et al., 1997; Helms and Johnson, 1998; Gowan et al., 2001; Wilson et al., 2008). We found in flat-mounted preparations that Lhx2 and Lhx9 were expressed in the dorsal midbrain, where cell bodies of commissural neurons reside (supplementary material Fig. S3A-B′). Moreover, the

Development (2014) doi:10.1242/dev.102327

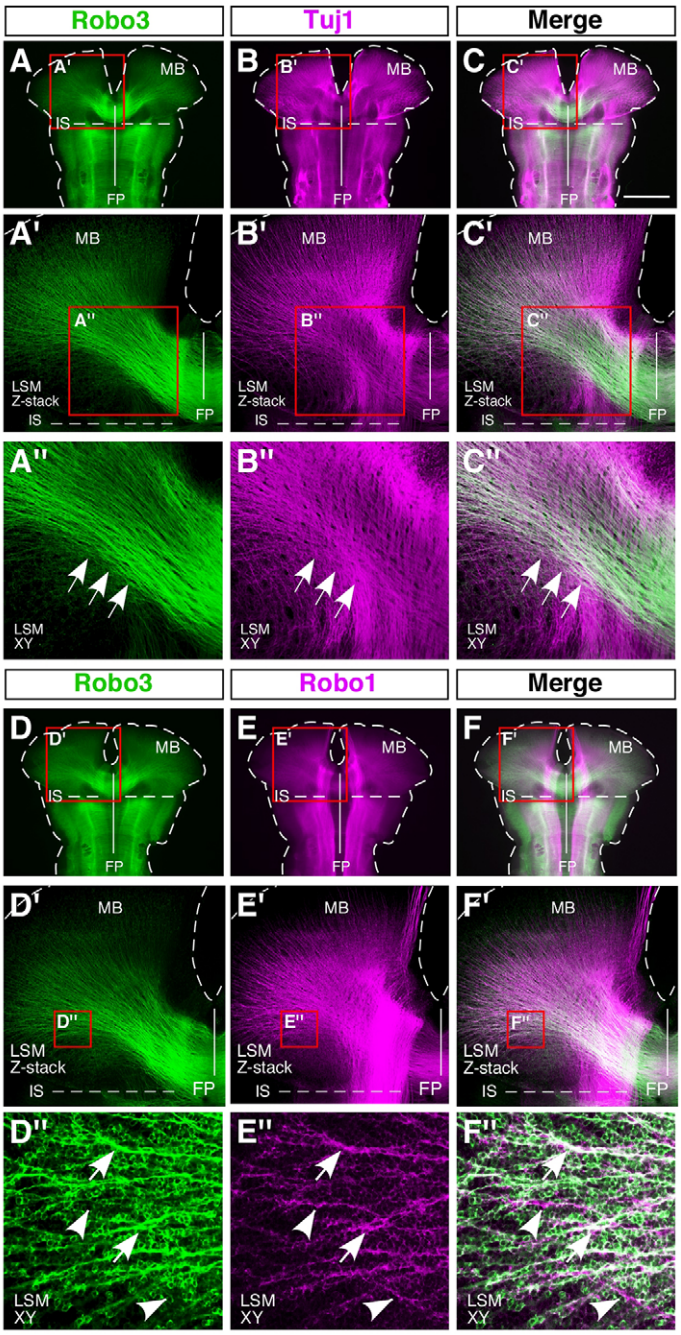

Fig. 2. Expression of Robo3 and Robo1 on midbrain commissural axons. (A-C″) Expression of Robo3 (A,A′,A″) and Tuj1 (B,B′,B″) in flat-mounted preparations at E11.5. (A′,B′,C′) Higher-magnification images of red rectangles in A,B,C, respectively, but showing a *z*-stack image of 18 optical sections (5 µm thickness) obtained by confocal LSM. (A″,B″,C″) High-power views of red rectangles in A′,B′,C′, respectively, but showing an *xy*-plane of LSM image. Robo3 is selectively expressed on commissural axons (arrows). (D-F″) Robo3 and Robo1 immunostaining similarly analyzed in A-C″. (D′,E′,F′) High-power images of red rectangles in D-F, respectively, but showing a *z*-stack image of LSM optical sections. (D″,E″,F″) Higher-magnification views of red rectangles in D′,E′,F′, respectively, but showing an *xy*-plane of LSM image. Note that pre-crossing segment of commissural axons expresses Robo3 and Robo1 (arrows). Robo3-negative ipsilateral axons also express Robo1 (arrowheads). Scale bar: 910 µm in A-F; 300 µm in A′-F′; 150 µm in A″-C″; 50 µm in D″-F″. FP, floor plate; IS, isthmus; LSM, laser scanning microscopy; MB, midbrain.

POU transcription factor Brn3a (Pou4f1 – Mouse Genome Informatics), a definitive marker of midbrain ipsilateral neurons (Fedtsova and Turner, 1995; Fedtsova et al., 2008), was also expressed in the dorsal midbrain (supplementary material Fig. S3C,C′). To characterize the expression of these molecules in more detail, we employed immunohistochemistry on transverse cryostat sections of the dorsal midbrain. We found that, among Lhx2-positive postmitotic cells (supplementary material Fig. S3D-I), there were two subclasses categorized by the presence or absence of Robo3 (Fig. 3A-C′). This is reminiscent of the observation in the spinal cord in which Lhx2 is expressed not only in dI1 commissural neurons but also in dI1 ipsilateral neurons (Wilson et al., 2008). We therefore asked whether the Lhx2-positive population in the dorsal midbrain encompasses ipsilateral neurons by focusing on the expression of Brn3a. We found that cells that were positive for Lhx2 also expressed Brn3a (Fig. 3D-F′). Importantly, Brn3a-positive cells never expressed Robo3 (Fig. 3G-I; supplementary material Fig. S4A-C). These results therefore indicate that, in the dorsal midbrain, Lhx2 is expressed not just in Robo3-positive commissural neurons but also in ipsilateral neurons. We also found that Lhx9 was expressed in the dorsal midbrain, and this Lhx9-positive population similarly included Brn3a-positive and Brn3a-negative cells (supplementary material Fig. S3J-L).

Thus, in subsequent analyses, we have used these expression profiles to distinguish between commissural and ipsilateral neurons in the dorsal midbrain.

Dbx1 is expressed by a subset of neural progenitors in the dorsal midbrain

To identify a crucial genetic determinant that triggers downstream molecular programs required for midline crossing by commissural neurons, we searched for transcription factors whose expression has been reported in the dorsal midbrain. Here, we focused on the homeodomain transcription factor Dbx1, because it has been shown that *Dbx1* mRNA is expressed by progenitor cells in the dorsal midbrain during the time when midbrain commissural neurons are generated (Mastick et al., 1997; Prakash et al., 2009). We first examined the overall expression pattern of Dbx1 in the midbrain using whole-mount immunohistochemistry on flat-mounted midbrain preparations at E11.5. As reported previously, we found that Dbx1 expression was restricted to the dorsal region of the midbrain (Fig. 4A). To characterize the Dbx1 expression in more detail, we next performed immunohistochemistry using transverse sections of the midbrain. We found that Dbx1 was expressed by progenitor cells, as judged by the expression of proliferation marker Ki67 (Mki67 – Mouse Genome Informatics) and postmitotic neuronal marker Tuj1 (Fig. 4B,D-I). Consistent with this, Dbx1-positive cells did not express postmitotically expressed molecules such as Lhx2 (Fig. 4J-L; supplementary material Fig. S4D-F). Moreover, among the progenitor cells, Dbx1 was expressed in subsets of cells positive for the proneural bHLH factor Ngn1 (Neurog1 – Mouse Genome Informatics) (Fig. 4B,C,M-O), but not in Ascl1-positive cells (Fig. 4P-R; supplementary material Fig. S4G-I). A similar Dbx1 expression pattern was also observed at E10.75 (supplementary material Fig. S5). Thus, these results raise the possibility that Dbx1 is involved in the generation of unique subsets of cells in the developing dorsal midbrain.

Dbx1 enhancer element reveals axonal trajectory of commissural neurons

Next, to examine which neuronal class employs Dbx1-mediated transcriptional program, we performed a lineage-tracing analysis

Development (2014) doi:10.1242/dev.102327

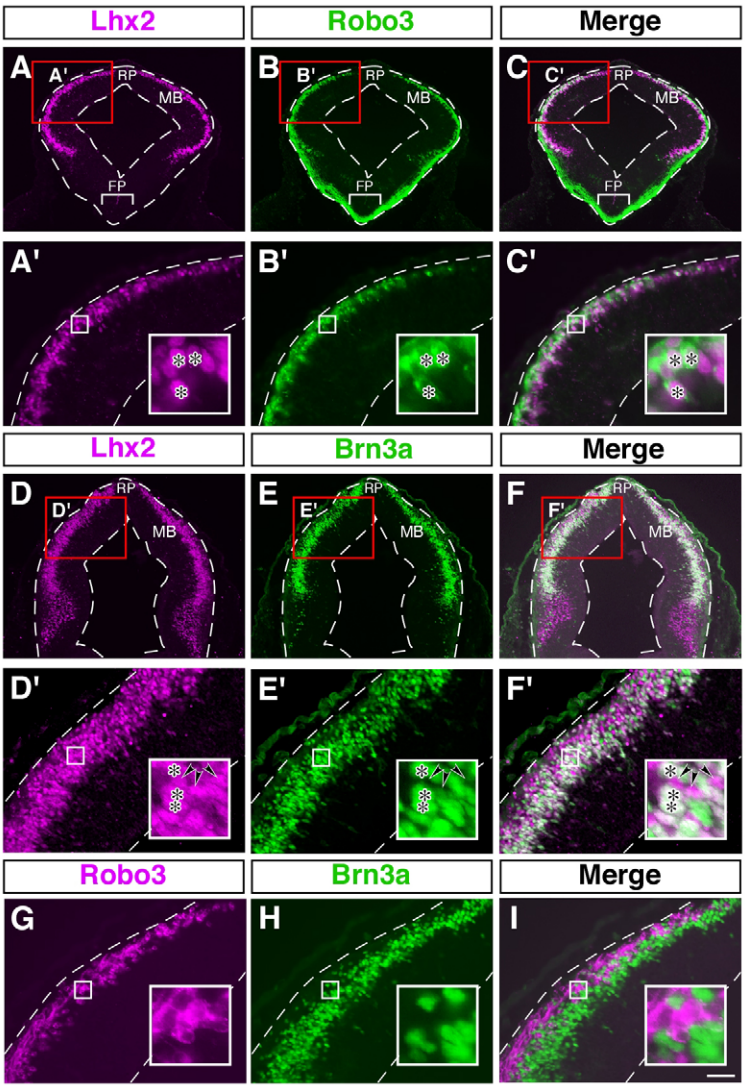

Fig. 3. Molecular profile of midbrain commissural neurons in the mouse. (A-I) Expression of Lhx2, Robo3 and Brn3a in transverse sections of E11.5 midbrain. (A′-F′) Higher-magnification images of the red boxes in A-F, respectively. (A-C′) The Lhx2-positive population consists of Robo3-positive and Robo3-negative cells. Asterisks represent cells double positive for Lhx2 and Robo3 (insets). (D-F′) Lhx2 is also expressed in Brn3a-positive cells. Asterisks indicate cells double positive for Lhx2 and Brn3a, and arrowheads indicate Lhx2-positive/Brn3a-negative cells (insets). (G-I) Robo3-positive cells are segregated from Brn3a-positive cells. Small boxes in A′-F′,G-I indicate regions enlarged in insets. Scale bar: 150 μm in A-F; 50 μm in A′-F′,G-I. FP, floor plate; MB, midbrain; RP, roof plate.

using the *Dbx1*-enhancer element. It has been shown that a distal 3.5 kb of the 5.7 kb *Dbx1* regulatory sequence acts as an enhancer element that controls unique expression of Dbx1 in the forebrain, midbrain, hindbrain and spinal cord (Lu et al., 1996). We therefore used this unique enhancer to generate an expression vector in which ZsGreen expression is under the control of the *Dbx1* enhancer. We then electroporated *Dbx1* enhancer-driven *ZsGreen1* (*Dbx1 enhancer::ZsGreen*) vector into the dorsal midbrain at E10.75, because at this stage both commissural and ipsilateral neurons can be transfected by our *in vivo* electroporation technique in mice (Fig. 1B,B′). We found in the electroporated embryos that axons growing toward the floor plate were selectively labeled with ZsGreen (Fig. 5A,A′). In addition, these ZsGreen-expressing commissural axons also expressed Robo3 (Fig. 5A-C′), indicating that Dbx1-positive progenitors in the dorsal midbrain give rise to Robo3-positive commissural neurons. Furthermore, expression analyses using transverse sections of the electroporated midbrain revealed that ZsGreen-positive postmitotic cells expressed Robo3, but did not express ipsilateral neuron marker Brn3a (Fig. 5D-L; supplementary material Fig. S4J-L). Together, these results therefore suggest that commissural neurons in the dorsal midbrain are generated selectively from Dbx1-positive progenitors.

Dbx1-triggered transcriptional program controls midline crossing by commissural axons

To test whether the downstream transcriptional program initiated by Dbx1 ultimately regulates midline crossing by midbrain commissural axons, we first performed Dbx1 gain-of-function experiments by ectopically expressing Dbx1 in progenitors of ipsilateral neurons. For this, we first took advantage of the fact that cells mainly transfected by *in vivo* electroporation at E11.5 are ipsilateral neurons (Fig. 1C,C′). We found that Dbx1 misexpression in the dorsal midbrain at this stage dramatically increased midline-crossing axons compared with controls (Fig. 6A-B′,H; supplementary material Figs S6 and S7). We also found that *Dbx1* electroporation at E10.75, the stage when both commissural and ipsilateral neurons are abundantly labeled by the electroporation (Fig. 1B,B′), resulted in more effective induction of midline-crossing axons at the expense of ipsilateral axons (Fig. 6C-D′,I).

Next, we carried out Dbx1 loss-of-function experiments using *in vivo* electroporation at E10.75. For this, we first misexpressed a dominant-negative form of Dbx1 (dnDbx1) in the dorsal midbrain. We found that expression of dnDbx1 caused loss of midline crossing without affecting caudally directed axon growth (Fig. 6E,E′,I). We next performed Dbx1 knockdown by introduction of siRNA specifically targeting *Dbx1*, and found that this similarly caused an

Development (2014) doi:10.1242/dev.102327

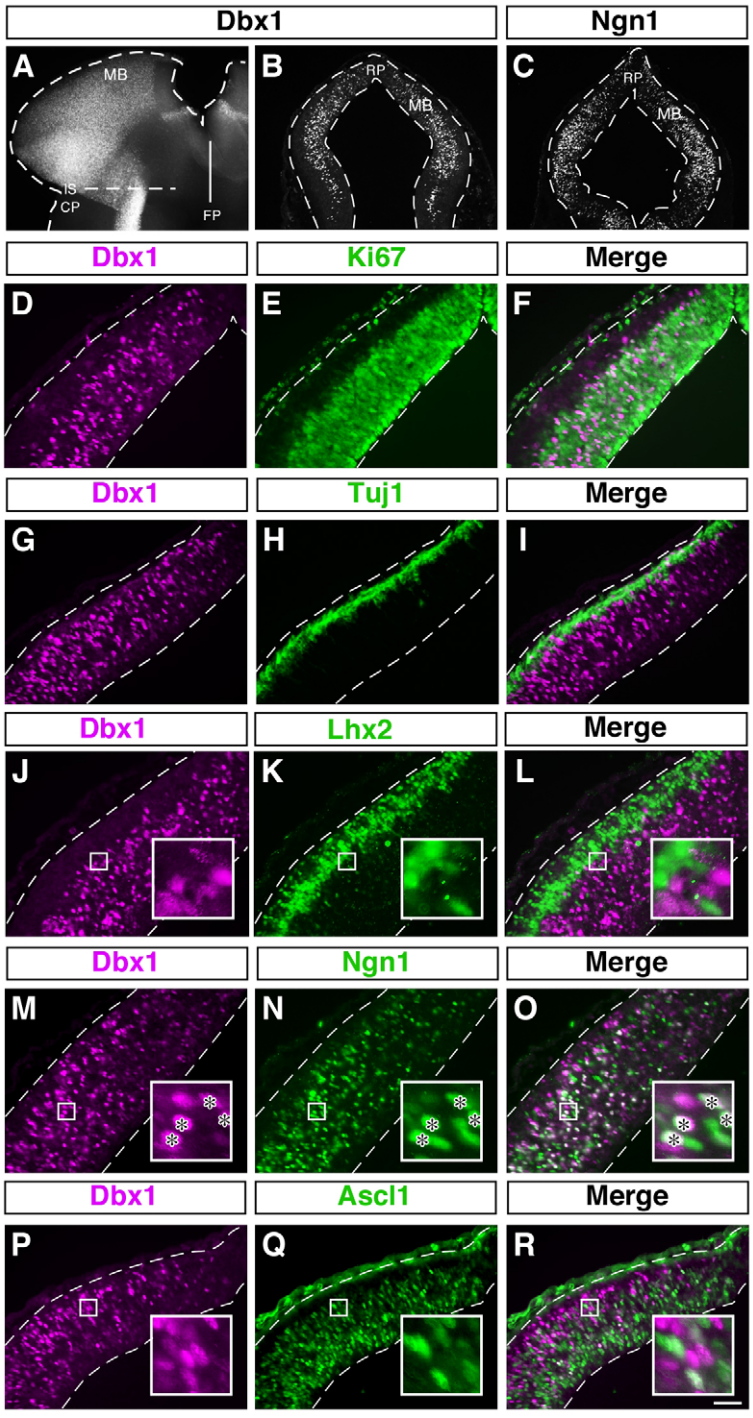

Fig. 4. Dbx1 is expressed by a subset of progenitor cells in the dorsal midbrain. (A) Dbx1 expression in flat-mounted preparations at E11.5. (B-R) Expression analyses in transverse sections of the dorsal midbrain at E11.5. (B,C) Expression of Dbx1 and Ngn1 in the midbrain. (D-I) Dbx1 is expressed by proliferating progenitors, as revealed by the expression analyses of Ki67 and Tuj1. (J-L) Dbx1 expression is not overlapped with that of postmitotically expressed Lhx2. (M-O) Expression of Dbx1 in subsets of Ngn1-positive cells. Asterisks in insets show cells double positive for Dbx1 and Ngn1. (P-R) Dbx1-positive cells are segregated from Ascl1-positive cells. Small boxes in J-R indicate areas enlarged in insets. Scale bar: 250 µm in A; 150 µm in B,C; 50 µm in D-R. CP, cerebellar plate; FP, floor plate; IS, isthmus; MB, midbrain; RP, roof plate.

absence of midline crossing (Fig. 6F,F′,J; supplementary material Fig. S8). In addition, the loss of midline crossing observed in the *Dbx1*-siRNA electroporated embryos was rescued by co-introduction of the siRNA-resistant variant of *Dbx1* (Fig. 6G,G′,J).

Together, these results therefore suggest that the expression of Dbx1 is necessary and sufficient to trigger downstream molecular programs required for midline crossing by midbrain commissural axons.

Suppression of ipsilateral neuron genetic program by Dbx1

To examine the molecular programs triggered by Dbx1, we next focused our attention on the expression of transcription factors that may be under the control of Dbx1. It has been shown in the chick ventral spinal cord that Dbx1 misexpression promotes a switch in transcription factor profile from V1 ipsilateral to V0 commissural neurons by suppressing the expression of transcription factors unique to ipsilateral neurons (Pierani et al., 2001). This raises the possibility that an ectopic generation of commissural neurons in the Dbx1-misexpressed dorsal midbrain (Fig. 6) is induced at the expense of ipsilateral neuron generation. To test this, we examined the expression of Brn3a after *Dbx1* electroporation in the midbrain. We found that the expression of Brn3a was significantly repressed in the *Dbx1*-transfected cells compared with *GFP*-transfected controls (Fig. 7A-F,H). Consistent with this, when analyzed using whole-mount immunohistochemistry on flat-mounted preparations,

Development (2014) doi:10.1242/dev.102327

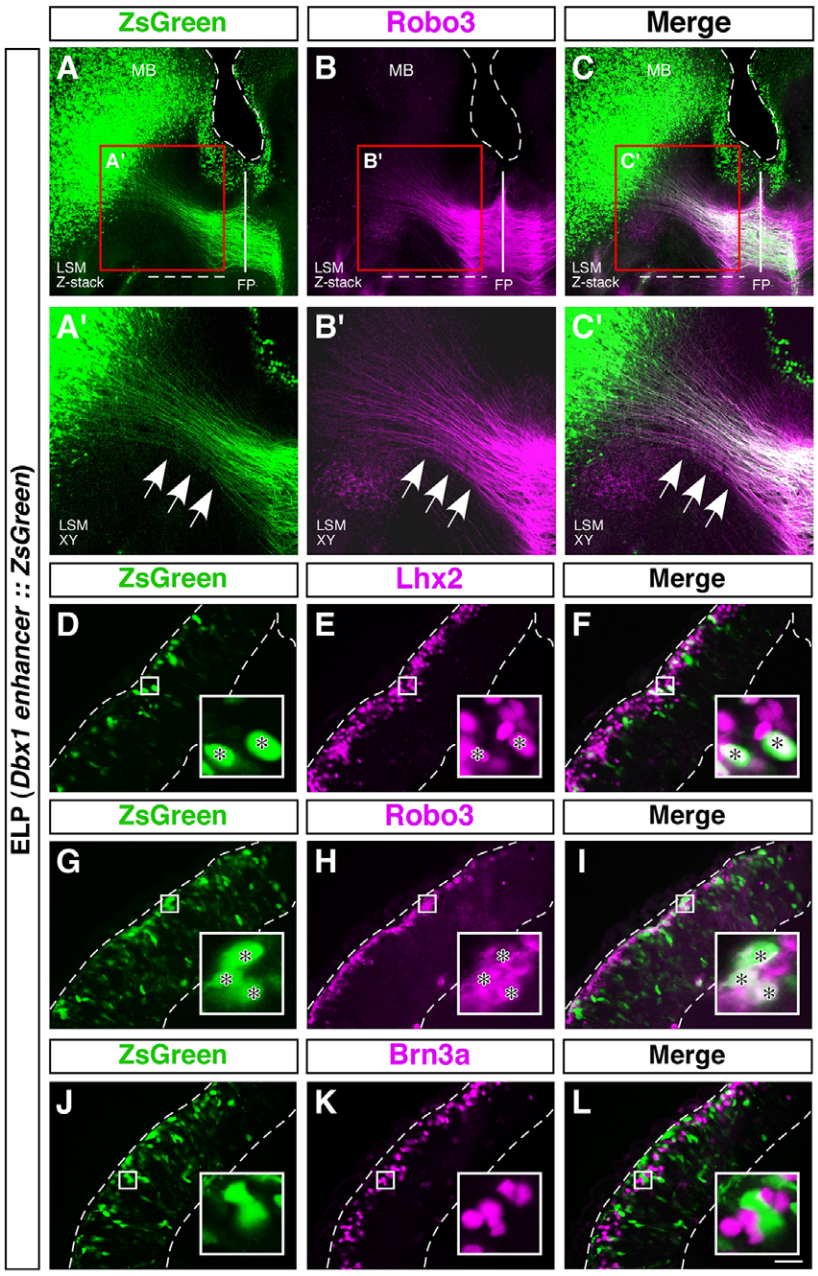

Fig. 5. Midbrain commissural neurons are derived from Dbx1-positive progenitors. (A-L) Cell-lineage tracing analyses using *Dbx1*-enhancer element. *In vivo* electroporation of *Dbx1 enhancer::ZsGreen* vector was performed at E10.75, and the expression of ZsGreen was analyzed. (A-C) *z*-stack LSM images of 31 optical sections (5 µm thickness) in flat-mounted preparations at E12.75. (A′-C′) Higher-magnification views of red boxes in A-C, respectively, but showing an *xy*-plane of LSM image. Axons growing toward the floor plate are selectively labeled by ZsGreen. Note that these labeled axons express Robo3 (arrows). (D-L) Molecular characterization of ZsGreen-positive cells in transverse sections. Electroporated midbrains were analyzed at E11.75, as an endogenous expression of Robo3 in the cell body declines at later developmental stages. (D-F) ZsGreen-labeled cells express Lhx2. The area of Lhx2-positive cells was employed to define the postmitotic zone in the dorsal midbrain. (G-I) ZsGreen-labeled cells in the postmitotic zone express Robo3 (asterisks in insets). (J-L) ZsGreen-positive cells in the postmitotic zone never express Brn3a. Small boxes in D-L indicate areas enlarged in insets. Scale bar: 160 µm in A-C; 80 µm in A′-C′; 50 µm in D-L. FP, floor plate; LSM, laser scanning microscopy; MB, midbrain.

Brn3a expression was dramatically suppressed in the *Dbx1*-electroporated area (Fig. 7G,G′). These results therefore suggest that the Dbx1-triggered transcriptional program may include suppression of ipsilateral neuron genetic programs to consolidate commissural neuron identity.

Homeodomain factor selectively expressed by midbrain commissural neurons

To further unravel the Dbx1-triggered transcriptional cascade, we next searched for a transcription factor that is selectively expressed in midbrain commissural neurons. In the dorsal midbrain, Lhx2 is expressed not only by commissural neurons but also by ipsilateral neurons (Fig. 3), suggesting that the expression of Lhx2 is not regulated within the Dbx1 cascade. Interestingly, it should be noted that, although V0 commissural neurons in the ventral spinal cord never express Lhx2 (Moran-Rivard et al., 2001), Dbx1 specifically activates the expression of homeodomain transcription factors Evx1/2 in V0 neurons (Pierani et al., 2001). Indeed, among the Evx gene family, it has been shown in the dorsal midbrain that Evx2 is expressed by cells with unknown characters (Dollé et al., 1994; Kmita et al., 2002). This prompted us to examine whether the expression of Evx2 is restricted to commissural neurons in the dorsal midbrain. We found that Evx2 was expressed by postmitotic cells in the dorsal midbrain (Fig. 8A-C; supplementary material Fig. S9), the expression of which did not overlap with that of Dbx1 expressed by progenitor cells (Fig. 8D-F; supplementary material Fig. S10A-C). In addition, the Evx2-positive population was a subset of Lhx2-positive cells (Fig. 8G-I). Strikingly, these Evx2-positive cells corresponded to Robo3-expressing cells (Fig. 8J-L; supplementary material Fig. S10D-F), and the expression of Evx2 never overlapped with that of the ipsilateral neuron marker Brn3a (Fig. 8M-O; supplementary material Fig. S10G-I). Together, these results indicate that Evx2 selectively marks Robo3-positive commissural neurons in the dorsal midbrain, thus raising the

Development (2014) doi:10.1242/dev.102327

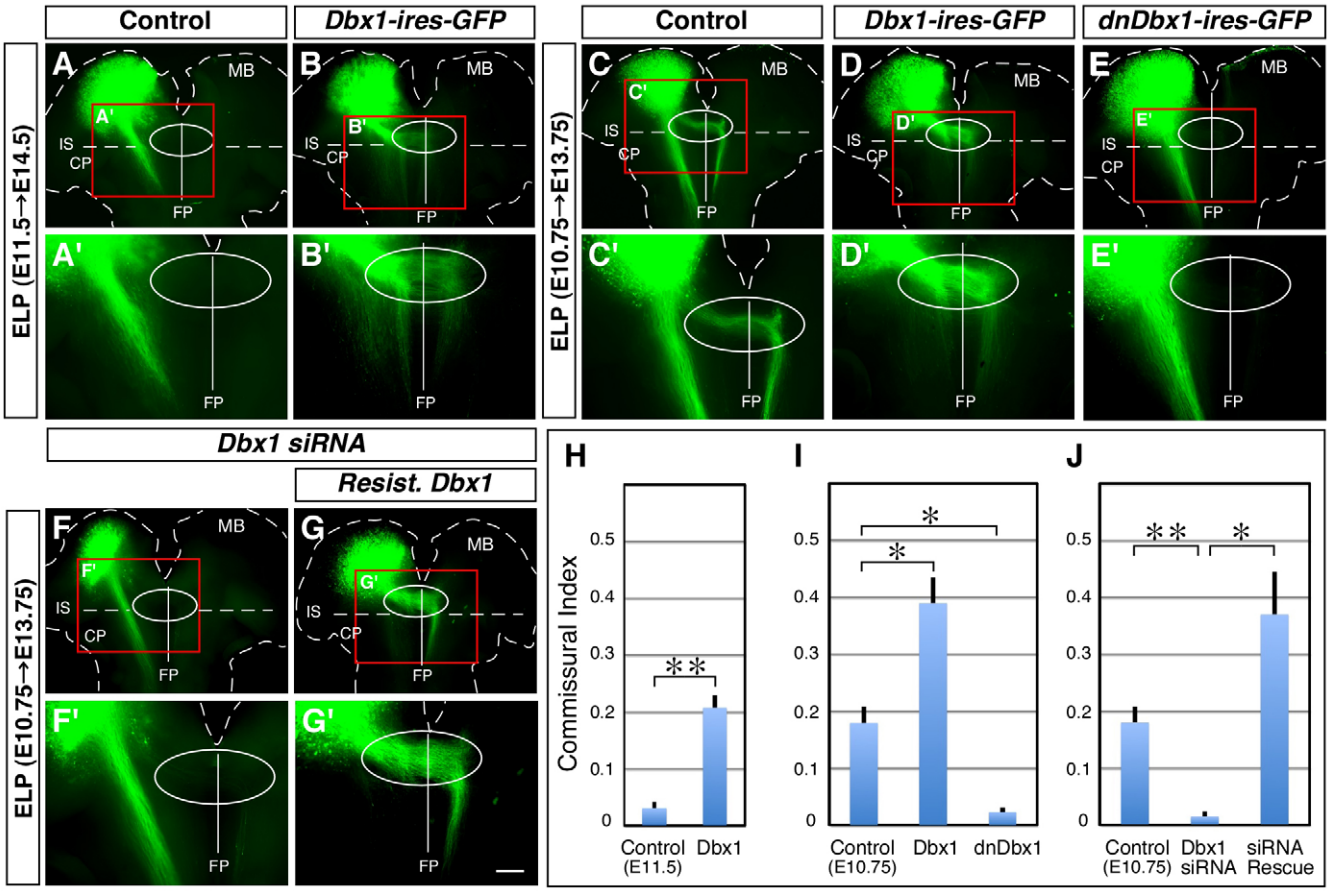

Fig. 6. The Dbx1-triggered transcriptional program is necessary and sufficient for midline crossing. (A,A′) Trajectory of GFP-labeled axons in controls (*n*=10). The GFP-expression vector was electroporated at E11.5. The majority labeled by GFP are ipsilateral axons. (B,B′) Electroporation of *Dbx1* (*Dbx1-ires-GFP*) at E11.5 dramatically increases midline-crossing axons (*n*=7). (C,C′) Trajectory of GFP-labeled axons in controls, but *in vivo* electroporation was performed at E10.75 (*n*=8). Both commissural and ipsilateral axons are labeled. (D,D′) Prominent induction of midline crossing by Dbx1 misexpression at the expense of ipsilateral axons. In these embryos, the electroporation of *Dbx1* was performed at E10.75 (*n*=4). (E,E′) Loss-of-function of Dbx1 using dnDbx1. The electroporation of *dnDbx1* was carried out at E10.75 (*n*=5). This causes loss of midline-crossing axons. (F,F′) Dbx1 knockdown by siRNA electroporation at E10.75 also results in loss of midline-crossing axons (*n*=6). (G,G′) Loss of midline-crossing phenotype caused by the *Dbx1* siRNA is rescued by co-introduction of the siRNA-resistant variant of *Dbx1* (*Resist. Dbx1*) (*n*=5). (A′-G′) Higher-magnification views of red rectangles in A-G, respectively. (A-G′) The white oval denotes the area around the ventral midbrain tegmentum that includes the floor plate. (H-J) Quantification of midline crossing evaluated by commissural index. Error bars indicate s.e.m. Statistical significance was determined by Mann-Whitney U-test, with a Bonferroni correction when appropriate (*P<0.05, **P<0.01). Scale bar: 500 μm in A-G; 250 μm in A′-G′. CP, cerebellar plate; FP, floor plate; IS, isthmus; MB, midbrain.

possibility that Evx2 is one of the transcription factors acting downstream of Dbx1.

Robo3 is an essential regulator for midline crossing within the Dbx1-triggered transcriptional program

Next, we directly addressed whether the expression of Robo3 is a crucial outcome regulated within the Dbx1-triggered transcriptional cascade. For this, we employed a misexpression (gain-of-function) approach using *in vivo* electroporation. As expected, we found that the misexpression of Dbx1 in the dorsal midbrain induced an ectopic expression of Evx2 compared with the non-electroporated control side of the midbrain (Fig. 9A,A′; supplementary material Fig. S11). Furthermore, Evx2 misexpression elicited an ectopic expression of Robo3 in the electroporated region (Fig. 9B,B′; supplementary material Fig. S12). We then asked whether the expression of Robo3 is ultimately regulated by the Dbx1-triggered molecular program. We found that Robo3 expression was dramatically induced on the *Dbx1*-electroporated side compared with the control side (Fig. 9C,C′), on which endogenous expression of Robo3 was downregulated in the dorsal midbrain at this stage (Fig. 9B′,C′). Moreover, commissural axons generated by the *Dbx1* electroporation strongly expressed Robo3 when they grew toward the floor plate (Fig. 9C,C′, arrowheads). Together, these results therefore suggest that the transcriptional program triggered by Dbx1 at the progenitor stage eventually regulates the expression of Robo3 on midbrain commissural axons.

Finally, because the role of Robo3 expressed by midbrain commissural neurons has been unexplored, we examined whether Robo3 is required for midline crossing by midbrain commissural axons. To this end, we carried out Robo3 knockdown using *in vivo* electroporation of *Robo3*-specific siRNA (Chen et al., 2008). As expected, we found that midline crossing was strongly inhibited by the Robo3 loss of function (Fig. 9D-E′,G). The specificity of the siRNA effect was ascertained by a rescue experiment in which the midline-crossing defect was reversed by co-introduction of the siRNA-resistant variant of *Robo3* (Fig. 9D,D′,F,F′,G). Thus, these results indicate that Robo3 is essential for midline crossing by midbrain commissural axons (supplementary material Fig. S13).

Taken together, these gain- and loss-of-function analyses therefore demonstrate that a single progenitor homeodomain factor Dbx1 has

Development (2014) doi:10.1242/dev.102327

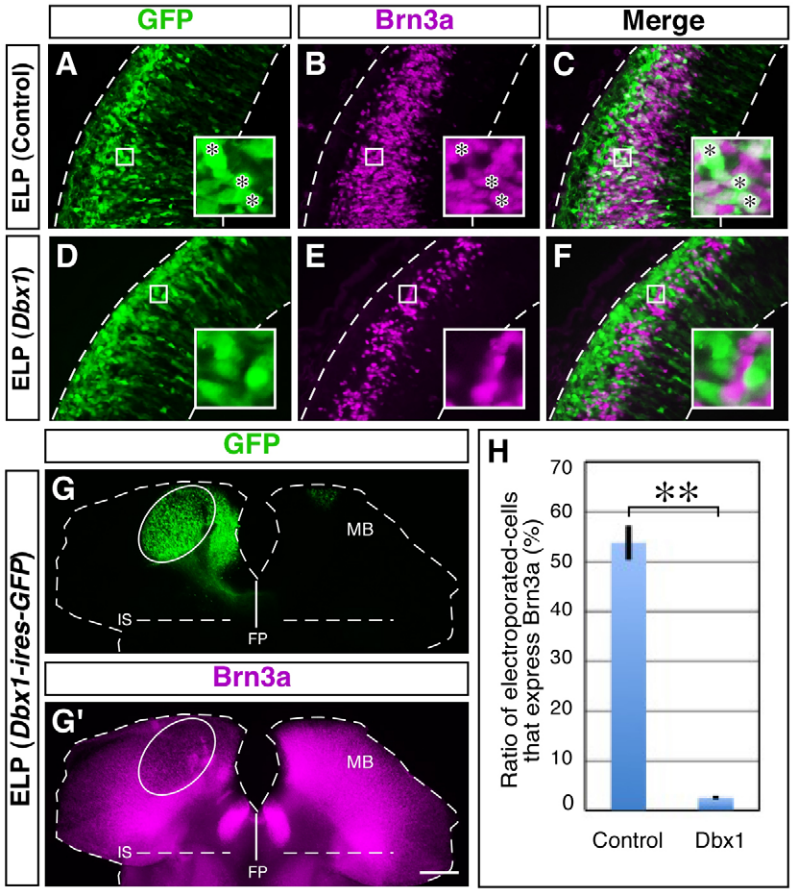

Fig. 7. Dbx1 represses Brn3a expression in midbrain ipsilateral neurons. (A-C) Expression of Brn3a in the dorsal midbrain of the control embryos (*n*=4). The GFP-expression vector was electroporated at E10.75, and the ratio of cells co-expressing GFP and Brn3a was analyzed in transverse sections at E12.75. Asterisks in insets show *GFP*-transfected cells that are also positive for Brn3a. (D-F) Expression of Brn3a in the dorsal midbrain, in which *Dbx1-ires-GFP* was electroporated (*n*=5). Note that GFP-positive cells do not express Brn3a (insets). (G,G′) Suppression of Brn3a expression elicited by Dbx1 misexpression in flat-mounted preparations. In the *Dbx1*-electroporated area (white oval), Brn3a expression is downregulated compared with that on the opposite side of the midbrain. (H) Quantification of suppression of Brn3a expression induced by Dbx1. The ratio of Brn3a-positive cells to GFP-expressing cells was calculated (**P<0.01, Student's t-test). Small boxes in A-F indicate areas enlarged in insets. Error bars indicate s.e.m. Scale bar: 70 μm in A-F; 400 μm in G,G′. FP, floor plate; IS, isthmus; MB, midbrain.

a crucial role in assigning midline-crossing identity by activating the downstream molecular programs that ultimately control the expression of Robo3 in midbrain commissural neurons.

DISCUSSION

A single progenitor transcription factor Dbx1 assigns midline-crossing identity

In the developing nervous system, unique expression of transcription factors ultimately determines the axonal projection patterns of individual neurons by directing the expression of specific guidance programs (Shirasaki and Pfaff, 2002; Polleux et al., 2007). Although commissural neurons in the vertebrate and invertebrate central nervous system have provided us with a wealth of information on the molecular mechanism of axon guidance (Dickson and Gilestro, 2006; Evans and Bashaw, 2010; Nawabi and Castellani, 2011), knowledge of the intrinsic genetic programs employed is still limited. For instance, it has remained obscure whether the action of a single transcription factor can activate downstream molecular programs required for midline crossing, or whether the parallel actions of several transcription factors are needed for this task. There has also been a crucial issue as to the timing of assignment of midline-crossing identity (e.g. at the progenitor stage or at the postmitotic stage). In this study, we show that a single transcription factor, Dbx1, expressed by progenitor cells in the dorsal midbrain acts as a crucial genetic determinant for midline-crossing identity. Interestingly, it should be noted that, in other classes of commissural neurons (e.g. spinal commissural neurons, contralateral RGCs, and cortical callosal neurons), the identity of 'cross or not to cross' seems to be assigned at the postmitotic stage (Herrera et al., 2003; Pak et al., 2004; Alcamo et al., 2008; Britanova et al., 2008; Wilson et al., 2008; Ding et al., 2012). Thus, our findings reveal the existence of a novel regulatory layer within the transcriptional cascade that contributes to the establishment of the wiring laterality of the developing nervous system.

Transcriptional control of binary fate decision between commissural and ipsilateral neurons

Our results show that molecular programs triggered by the progenitor transcription factor Dbx1 are necessary and sufficient to confer midline-crossing identity in the developing midbrain. Strikingly, Dbx1 misexpression resulted in an ectopic generation of Robo3-positive commissural neurons at the expense of ipsilateral neuron differentiation, as represented by suppression of the expression of Brn3a, an ipsilateral neuron marker in the midbrain. This suggests that, by activating several molecular programs in parallel, Dbx1 has a crucial role not only in promoting the specification of commissural neuron identity but also in suppressing the expression of ipsilateral neuron character, which may contribute to consolidating the identity of commissural neurons in the dorsal midbrain. In this context, it is noteworthy that many of the transcription factors possessing a role for fate specification have repressive function toward cells with contrasting characteristics (Arber et al., 1999; Thaler et al., 1999; Moran-Rivard et al., 2001; Pierani et al., 2001). For example, among dI1-class dorsal interneurons in the spinal cord, Barhl2 has been shown to facilitate differentiation of ipsilateral neurons by selectively suppressing the features of commissural neurons (Ding et al., 2012). Likewise, during neocortical development, Satb2 acts as a genetic determinant of callosal projection neurons by repressing the expression of Ctip2 (Bcl11b – Mouse Genome Informatics), a crucial factor for specification of subcortical projection neuron identity

Development (2014) doi:10.1242/dev.102327

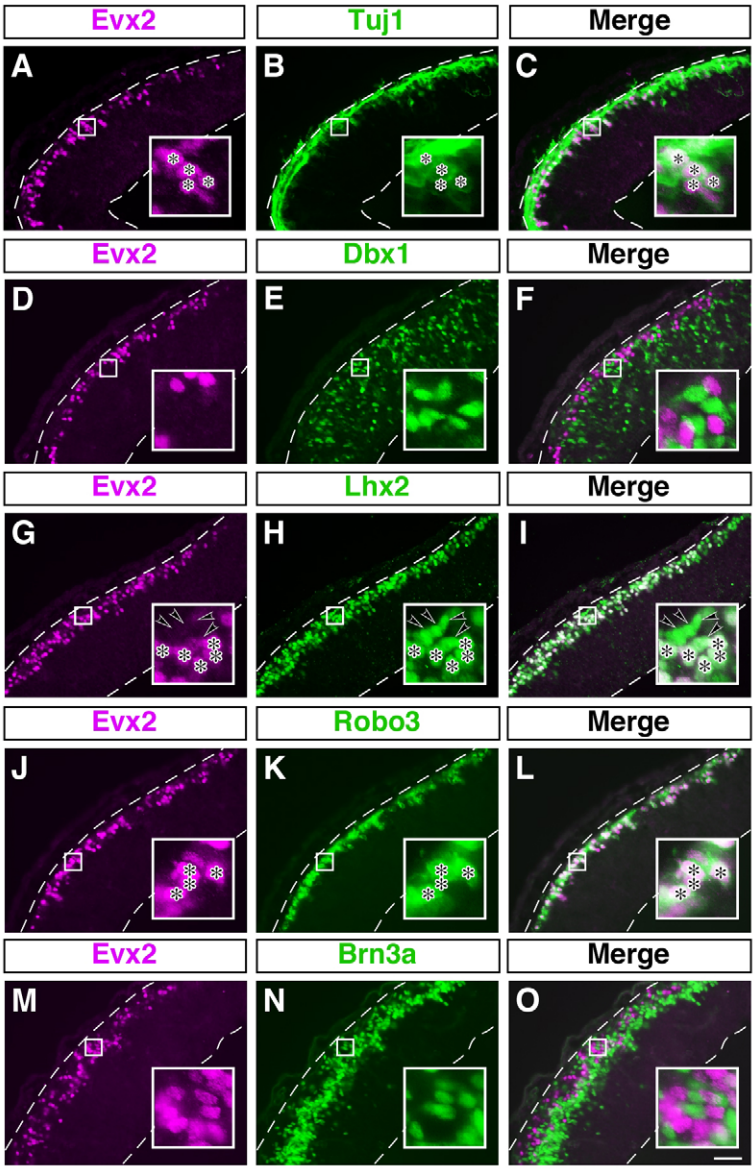

Fig. 8. Evx2 expression is restricted to midbrain commissural neurons. (A-C) Evx2 is expressed by postmitotic neurons in the dorsal midbrain, as revealed by double-label immunohistochemistry of Evx2 and Tuj1 in transverse sections of E11.5 midbrain. Asterisks show cells double positive for Evx2 and Tuj1 (insets). (D-F) Colocalization of Evx2 and Dbx1 is not observed. (G-I) Evx2 is expressed by a subset of Lhx2-positive cells. Asterisks represent cells double positive for Evx2 and Lhx2, whereas arrowheads depict Lhx2-positive/Evx2-negative cells (insets). (J-L) Evx2-positive cells correspond to Robo3-expressing cells. Asterisks show cells co-expressing Evx2 and Robo3 (insets). (M-O) Evx2-positive cells are segregated from Brn3a-expressing cells. Small boxes in A-O indicate regions enlarged in insets. Scale bar: 50 μm.

(Alcamo et al., 2008; Britanova et al., 2008). Thus, at least in some cellular contexts, the repressive function of the dedicated transcription factors may represent one broadly applicable strategy for the binary fate decision between commissural and ipsilateral neurons in order to restrain the potential to express conflicting genetic programs during development.

Dbx1 triggers molecular programs that ultimately induce Robo3 expression

In the developing ventral spinal cord, it has been shown that Dbx1 is specifically expressed by a subset of progenitor cells that give rise to commissural neurons (V0 interneurons) (Pierani et al., 1999; Pierani et al., 2001). In addition, in *Dbx1* mutant mice, the progenitor cells fail to generate V0 commissural neurons (Pierani et al., 2001). These findings suggest that Dbx1 is required for the generation of a subset of ventral commissural neurons in the spinal cord. However, it remains to be determined whether the expression of Dbx1 alone is sufficient to activate downstream molecular programs that directly couple with the expression of guidance programs for midline crossing. In the present study, we show that Dbx1-activated molecular programs ultimately induce the expression of Robo3 on midbrain commissural axons, which is hierarchically regulated via the expression of Evx2 at the postmitotic stage. Furthermore, we also show that the midline crossing by midbrain commissural axons depends crucially on the expression of Robo3. Interestingly, similar molecular program is also the case with dI1 commissural neurons generated from Atoh1-expressing progenitors in the dorsal spinal cord, although the expression of Robo3 is controlled by Lhx2 and Lhx9 at the postmitotic stage (Wilson et al., 2008). Because all classes of commissural axons in the spinal cord are misrouted and fail to cross the floor plate in *Robo3* mutant mice (Sabatier et al., 2004; Wilson et al., 2008), it is predicted that axon guidance programs employed by V0 commissural neurons should also include the expression of Robo3. Thus, although upstream transcriptional programs for commissural neuron differentiation seem different among commissural neuron classes, we speculate that one of the essential outcomes from these molecular programs is to activate the expression of Robo3 to silence Slit-Robo1 repulsive signaling when commissural axons approach and cross the floor plate.

Development (2014) doi:10.1242/dev.102327

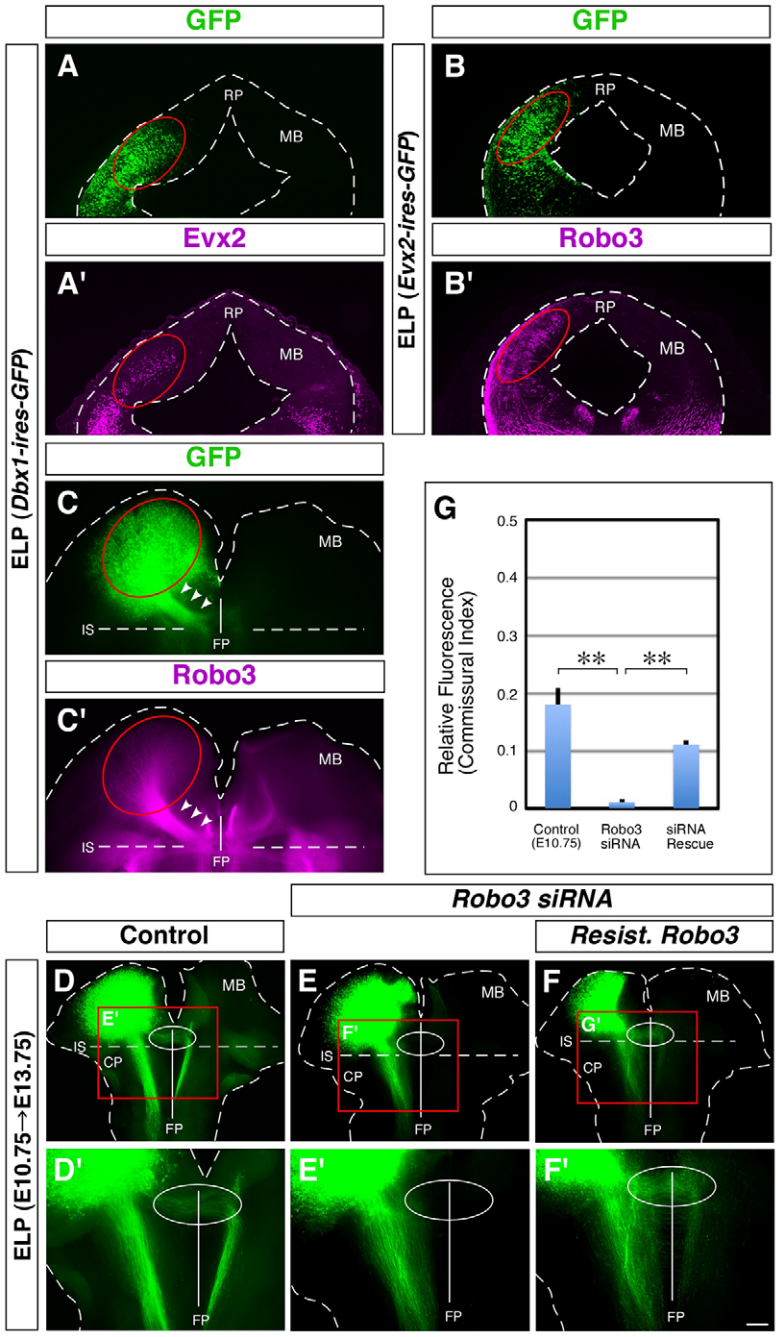

Fig. 9. Robo3 as a crucial downstream effector of Dbx1-triggered transcriptional program. (A,A′) Misexpression of Dbx1 induces an ectopic expression of Evx2. Electroporation of *Dbx1* (*Dbx1-ires-GFP*) was performed at E11.5, and the electroporated midbrains were analyzed for expression of Evx2 in transverse sections at E13.5. (B,B′) Misexpression of Evx2 at E11.5 induces an ectopic expression of Robo3. *Evx2*-electroporated midbrains were analyzed for expression of Robo3 at E13.5. (C,C′) Misexpression of Dbx1 at E11.5 dramatically induces Robo3 expression on commissural axons, as revealed by Robo3 labeling in flat-mounted preparations at E13.5. Arrowheads denote Robo3-expressing commissural axons that were ectopically generated by *Dbx1* electroporation. (A-C′) Red ovals indicate electroporated areas. (D,D′) Trajectory of GFP-labeled axons in controls (*n*=8). Because the electroporation was performed at E10.75, commissural as well as ipsilateral axons are labeled (see also Fig. 1B,B′). (E,E′) Loss-of-function of Robo3 by siRNA-mediated knockdown inhibits midline crossing. Co-electroporation of *Robo3* siRNA and *GFP* was performed at E10.75 (*n*=8). (F,F′) Midline-crossing defect caused by *Robo3* siRNA is rescued by co-introduction of the siRNA-resistant variant of *Robo3* (*Resist. Robo3*) (*n*=11). (D′,E′,F′) Higher magnification views of red rectangles in D,E,F, respectively. (D-F′) White oval denotes area around the ventral midbrain tegmentum that includes the floor plate. (G) Quantification of midline crossing evaluated by commissural index (**P<0.01, Mann-Whitney U-test with a Bonferroni correction). Error bars indicate s.e.m. Scale bar: 140 μm in A-B′; 280 μm in C-C′; D-F in 400 μm; 200 μm in D′-F′. CP, cerebellar plate; FP, floor plate; IS, isthmus; MB, midbrain; RP, roof plate.

A unique feature expressed by midbrain commissural neurons

Our lineage-tracing studies revealed that axons of midbrain commissural neurons generated from Dbx1-expressing progenitor cells grow caudally after crossing the floor plate, as opposed to axonal behavior of V0 commissural neurons generated from Dbx1-postive progenitor cells in the ventral spinal cord (Moran-Rivard et al., 2001; Pierani et al., 2001). Interestingly, in the ventral spinal cord of *Dbx1* mutant mice, it has been shown that the molecular program for rostrally directed axon growth by V0 neurons is under the control of Dbx1-triggered transcriptional programs (Pierani et al., 2001). However, this is in a sharp contrast with transcriptional program employed by midbrain commissural neurons, since these midbrain axons still grow caudally under conditions where Dbx1 function is lost (Fig. 6). In addition, ipsilateral neurons in the dorsal midbrain that are independent of Dbx1-triggered genetic programs also extend axons caudally (Fig. 1). It is therefore likely that a unique transcriptional program acting independently of Dbx1 directs the expression of molecular programs required for caudally oriented axon growth. Whether this transcriptional program is triggered by the action of a single dedicated transcription factor or by the parallel actions of several transcription factors remains to be determined.

MATERIALS AND METHODS

Mice

Timed pregnant Institute for Cancer Research (ICR) mice were obtained from Japan SLC (Hamamatsu, Japan). Noon of the day on which a vaginal plug was found was designated as embryonic day 0.5 (E0.5). All experiments were performed in accordance with the guidelines of the animal welfare committees of Osaka University and the Japan Neuroscience Society.

Development (2014) doi:10.1242/dev.102327

In vivo electroporation

In vivo electroporation in mice was performed as described (Saba et al., 2003; Saito, 2006). In brief, after plasmid DNA was injected into the canal of the midbrain, electric pulses were applied to the dorsal midbrain using square pulse electroporator (CUY-21, Bex) with a pair of 1 mm diameter platinum electrode (CUY650P1, Nepa Gene). For cell-lineage-tracing analyses in transverse cryostat sections, we used a pair of 3 mm diameter electrode (CUY650P3, Nepa Gene) to electroporate the *Dbx1*-enhancer vector into a large area of the dorsal midbrain. Two to 3 days after electroporation, the embryos were taken out from the mother, fixed with 4% paraformaldehyde in 0.1 M phosphate buffer (pH 7.4) for 2 hours at 4°C and subjected to immunohistochemistry for further analyses.

Immunohistochemistry

Whole-mount immunohistochemistry on flat-mounted midbrain/hindbrain preparations was performed as described (Shirasaki et al., 2006). The flat-mounted preparations enable ready recognition of the entire trajectories of labeled axons. The procedure for flat-mounted midbrain/hindbrain preparation was described previously (Shirasaki et al., 1995). Immunostaining was also carried out on 12 µm-thick transverse cryostat sections of the midbrain as described (Shirasaki et al., 2006). Commercially available primary antibodies used are listed in supplementary material Table S1. Primary antibody against mouse Dbx1 was generated in rabbits using a keyhole limpet hemocyanin (KLH)-conjugated peptide containing the 15 amino acids of the mouse Dbx1 (CDEDEEGEEDEEITVS) (Vue et al., 2007). An Evx2 guinea pig polyclonal antibody was generated using a KLH-conjugated peptide that includes 20 amino acids of the mouse Evx2 (EIASATESRKKPSHYSEAAAC), the amino acid sequence of which is unique to Evx2 among the Evx-class homeodomain proteins. The Vector MOM Immunodetection Kit (Vector Laboratories) was used when primary antibodies from mouse were used. Images were taken by a fluorescence microscope (Olympus, BX61N) with a high-resolution digital cooled charge-coupled device (CCD) camera (Hamamatsu Photonics, ORCA-AG) and by a confocal laser scanning microscope (Olympus, Fluoview FV300).

Plasmid construction

To visualize trajectory of GFP-labeled axons from the dorsal midbrain, we first constructed a pCAGGS-AcGFP1 vector. Briefly, an open reading frame (ORF) of *AcGFP1* was amplified from pIRES2-AcGFP1 vector (Clontech) by PCR and cloned into the *Eco*RI sites of pCAGGS vector (Niwa et al., 1991). For gain- and loss-of-function experiments, pCAGGS-IRES2-AcGFP1 vector was generated. For this, a fragment containing *IRES2-AcGFP1* was isolated from pIRES2-AcGFP1 (Clontech) by digesting with *Xho*I and *Not*I sites and inserted into the pCAGGS vector. For gain-of-function experiments for Dbx1 and Evx2, ORF clones of mouse *Dbx1* (GenBank accession no. BC082541) and human *Evx2* (GenBank accession no. NM_001080458) were obtained from Open Biosystems and OriGene, respectively. After an HA-tag was fused to the N-terminus of Dbx1 and Evx2, these fragments were subcloned into a pCAGGS-IRES2-AcGFP1 vector. To generate dnDbx1 for loss-of-function experiments, we fused the activation domain of the herpesvirus protein VP16 resides (amino acids 446-490) to the C-terminus of the Dbx1, and the *dnDbx1* fragment was subcloned into pCAGGS-IRES2-AcGFP1 vector. An ORF of human *Robo3* (GenBank accession no. BC008623) was purchased from Open Biosystems in order to generate an siRNA-resistant variant (see below). We fused Myc-tag to the C-terminus of Robo3 and inserted into the pCAGGS vector. For cell lineage-tracing analysis of Dbx1-positive progenitors, we utilized a distal 3.5 kb of the 5.7 kb *Dbx1* regulatory sequence as a *Dbx1* enhancer element (Lu et al., 1996). The 3.5 kb *Dbx1* enhancer was isolated from a *Mus musculus molossinus* (MSM) mouse bacterial artificial clone (BAC) clone that contains *Dbx1* gene (clone name: MSMg01-341M02, RIKEN BioResource Center DNA Bank) (Abe et al., 2004). Then we generated *Dbx1 enhancer::ZsGreen* vector to drive the expression of fluorescent protein ZsGreen1 (Clontech) under the control of minimum *β-globin* promoter combined with the *Dbx1* enhancer.

siRNA-mediated gene knockdown

Stealth siRNAs for mouse *Dbx1* were designed using BLOCK-iT RNAi Designer (Invitrogen). The sequences of the sense strand were: 5′-CCGGCCACUCUAGUUUCCUAGUAGA-3′, 5′-GGUAAACCGUCAG-ACUUCUCUGAUU-3′. Because both of these siRNAs yielded a similar axon guidance phenotype (Fig. 6F,F′; supplementary material Fig. S8), we routinely used the former for the loss-of-function and the rescue experiments. A Stealth siRNA for mouse *Robo3* was also designed using BLOCK-iT RNAi Designer. The target sequence and the specificity of *Robo3* siRNA were as described (Chen et al., 2008). The siRNA and plasmid DNA were co-electroporated as described above. In rescue experiments, to generate the siRNA resistant variants of *Dbx1* and *Robo3*, several silent mutations were introduced into the siRNA target regions using PrimeSTAR Mutagenesis Basal Kit (TaKaRa). The resistant sequences of the sense strand were: *Dbx1*, 5′-GUGGACAUAGCUCCUUUUUGG-UCGA-3′; *Robo3*, 5′-CUACUUGGUCAGGAUGGUUGAAAAU-3′.

Quantification of GFP-labeled axon behavior and transfected cell identity

Flat-mounted preparations were made from the electroporated embryos and immunostained with anti-GFP. Non-saturated fluorescent images were taken using a fluorescence microscope with a ×2 objective lens to capture overall trajectory of the labeled axons. Mean fluorescence intensity of cohort of commissural and ipsilateral axons at the isthmus (midbrain/hindbrain boundary) was measured using ImageJ software (Schneider et al., 2012). After mean fluorescence intensity of unstained (background) areas was subtracted, the ratio of commissural to ipsilateral axons was calculated, and then this ratio was defined as commissural index (Wilson et al., 2008).

To analyze the identity of *Dbx1*-transfected cells, the number of GFP-labeled cells and Brn3a-positive cells was counted on 12 µm-thick transverse cryosections of the dorsal midbrain using ImageJ software (Schneider et al., 2012). For this, a 150 µm square was placed on the Brn3a expression domain in the postmitotic layers of the dorsal midbrain, as the minimum vertical length of Brn3a-positive layers is approximately 150 µm at the embryonic stage examined. The ratio of Brn3a-positive cells to GFP-labeled cells within the square was then calculated. Three or four embryos of each experimental condition were used for the analysis.

Acknowledgements

We thank Fujio Murakami for anti-Robo3 and anti-Robo1 antibodies; Jun-ichi Miyazaki for pCAGGS vector; and Yusuke Kamachi for pCMV/SV2-HA vector. We are grateful to Nobuhiko Yamamoto for comments on the manuscript and encouragement of this work. We also thank members of the Shirasaki group for helpful comments. The mAb 99.1-3A2 developed by Thomas M. Jessell and Susan Brenner-Morton was obtained from the Developmental Studies Hybridoma Bank developed under the auspices of the NICHD and maintained by The University of Iowa, Department of Biology, Iowa City, IA 52242, USA.

Competing interests

The authors declare no competing financial interests.

Author contributions

Y.I. carried out the experiments. Y.I. and R.S. analyzed the data. Y.I. and R.S. designed experiments and interpreted results. Y.I. and R.S. wrote the paper. R.S. conceived and supervised the project.

Funding

This work was supported by Grant-in-Aid for Young Scientists (A) [18680028] and (S) [21670002] from the Japan Society for the Promotion of Science (JSPS KAKENHI); by the Uehara Memorial Foundation; the Takeda Science Foundation; and the Mitsubishi Foundation (to R.S.).

Supplementary material

Supplementary material available online at
http://dev.biologists.org/lookup/suppl/doi:10.1242/dev.102327/-/DC1

References

Abe, K., Noguchi, H., Tagawa, K., Yuzuriha, M., Toyoda, A., Kojima, T., Ezawa, K., Saitou, N., Hattori, M., Sakaki, Y. et al. (2004). Contribution of Asian mouse subspecies Mus musculus molossinus to genomic constitution of strain C57BL/6J, as defined by BAC-end sequence-SNP analysis. *Genome Res.* **14**, 2439-2447.

Alcamo, E. A., Chirivella, L., Dautzenberg, M., Dobreva, G., Fariñas, I., Grosschedl, R. and McConnell, S. K. (2008). Satb2 regulates callosal projection neuron identity in the developing cerebral cortex. *Neuron* **57**, 364-377.

Arber, S., Han, B., Mendelsohn, M., Smith, M., Jessell, T. M. and Sockanathan, S. (1999). Requirement for the homeobox gene Hb9 in the consolidation of motor neuron identity. *Neuron* **23**, 659-674.
Bermingham, N. A., Hassan, B. A., Wang, V. Y., Fernandez, M., Banfi, S., Bellen, H. J., Fritzsch, B. and Zoghbi, H. Y. (2001). Proprioceptor pathway development is dependent on Math1. *Neuron* **30**, 411-422.
Britanova, O., de Juan Romero, C., Cheung, A., Kwan, K. Y., Schwark, M., Gyorgy, A., Vogel, T., Akopov, S., Mitkovski, M., Agoston, D. et al. (2008). Satb2 is a postmitotic determinant for upper-layer neuron specification in the neocortex. *Neuron* **57**, 378-392.
Chen, Z., Gore, B. B., Long, H., Ma, L. and Tessier-Lavigne, M. (2008). Alternative splicing of the Robo3 axon guidance receptor governs the midline switch from attraction to repulsion. *Neuron* **58**, 325-332.
Dickson, B. J. and Gilestro, G. F. (2006). Regulation of commissural axon pathfinding by slit and its Robo receptors. *Annu. Rev. Cell Dev. Biol.* **22**, 651-675.
Ding, Q., Joshi, P. S., Xie, Z. H., Xiang, M. and Gan, L. (2012). BARHL2 transcription factor regulates the ipsilateral/contralateral subtype divergence in postmitotic dI1 neurons of the developing spinal cord. *Proc. Natl. Acad. Sci. USA* **109**, 1566-1571.
Dollé, P., Fraulob, V. and Duboule, D. (1994). Developmental expression of the mouse Evx-2 gene: relationship with the evolution of the HOM/Hox complex. *Development* **Suppl. 1994**, 143-153.
Evans, T. A. and Bashaw, G. J. (2010). Axon guidance at the midline: of mice and flies. *Curr. Opin. Neurobiol.* **20**, 79-85.
Fedtsova, N. G. and Turner, E. E. (1995). Brn-3.0 expression identifies early post-mitotic CNS neurons and sensory neural precursors. *Mech. Dev.* **53**, 291-304.
Fedtsova, N., Quina, L. A., Wang, S. and Turner, E. E. (2008). Regulation of the development of tectal neurons and their projections by transcription factors Brn3a and Pax7. *Dev. Biol.* **316**, 6-20.
García-Frigola, C., Carreres, M. I., Vegar, C., Mason, C. and Herrera, E. (2008). Zic2 promotes axonal divergence at the optic chiasm midline by EphB1-dependent and -independent mechanisms. *Development* **135**, 1833-1841.
Gowan, K., Helms, A. W., Hunsaker, T. L., Collisson, T., Ebert, P. J., Odom, R. and Johnson, J. E. (2001). Crossinhibitory activities of Ngn1 and Math1 allow specification of distinct dorsal interneurons. *Neuron* **31**, 219-232.
Helms, A. W. and Johnson, J. E. (1998). Progenitors of dorsal commissural interneurons are defined by MATH1 expression. *Development* **125**, 919-928.
Herrera, E., Brown, L., Aruga, J., Rachel, R. A., Dolen, G., Mikoshiba, K., Brown, S. and Mason, C. A. (2003). Zic2 patterns binocular vision by specifying the uncrossed retinal projection. *Cell* **114**, 545-557.
Kmita, M., Tarchini, B., Duboule, D. and Hérault, Y. (2002). Evolutionary conserved sequences are required for the insulation of the vertebrate Hoxd complex in neural cells. *Development* **129**, 5521-5528.
Kröger, S. and Schwarz, U. (1990). The avian tectobulbar tract: development, explant culture, and effects of antibodies on the pattern of neurite outgrowth. *J. Neurosci.* **10**, 3118-3134.
Lee, R., Petros, T. J. and Mason, C. A. (2008). Zic2 regulates retinal ganglion cell axon avoidance of ephrinB2 through inducing expression of the guidance receptor EphB1. *J. Neurosci.* **28**, 5910-5919.
Liem, K. F., Jr, Tremml, G. and Jessell, T. M. (1997). A role for the roof plate and its resident TGFbeta-related proteins in neuronal patterning in the dorsal spinal cord. *Cell* **91**, 127-138.
Lu, S., Shashikant, C. S. and Ruddle, F. H. (1996). Separate cis-acting elements determine the expression of mouse Dbx gene in multiple spatial domains of the central nervous system. *Mech. Dev.* **58**, 193-202.
Marillat, V., Sabatier, C., Failli, V., Matsunaga, E., Sotelo, C., Tessier-Lavigne, M. and Chédotal, A. (2004). The slit receptor Rig-1/Robo3 controls midline crossing by hindbrain precerebellar neurons and axons. *Neuron* **43**, 69-79.
Mastick, G. S. and Easter, S. S., Jr (1996). Initial organization of neurons and tracts in the embryonic mouse fore- and midbrain. *Dev. Biol.* **173**, 79-94.
Mastick, G. S., Davis, N. M., Andrew, G. L. and Easter, S. S., Jr (1997). Pax-6 functions in boundary formation and axon guidance in the embryonic mouse forebrain. *Development* **124**, 1985-1997.
Moran-Rivard, L., Kagawa, T., Saueressig, H., Gross, M. K., Burrill, J. and Goulding, M. (2001). Evx1 is a postmitotic determinant of v0 interneuron identity in the spinal cord. *Neuron* **29**, 385-399.
Murray, E. A. and Coulter, J. D. (1982). Organization of tectospinal neurons in the cat and rat superior colliculus. *Brain Res.* **243**, 201-214.
Nawabi, H. and Castellani, V. (2011). Axonal commissures in the central nervous system: how to cross the midline? *Cell. Mol. Life Sci.* **68**, 2539-2553.
Niwa, H., Yamamura, K. and Miyazaki, J. (1991). Efficient selection for high-expression transfectants with a novel eukaryotic vector. *Gene* **108**, 193-199.
Pak, W., Hindges, R., Lim, Y. S., Pfaff, S. L. and O'Leary, D. D. (2004). Magnitude of binocular vision controlled by islet-2 repression of a genetic program that specifies laterality of retinal axon pathfinding. *Cell* **119**, 567-578.
Pierani, A., Brenner-Morton, S., Chiang, C. and Jessell, T. M. (1999). A sonic hedgehog-independent, retinoid-activated pathway of neurogenesis in the ventral spinal cord. *Cell* **97**, 903-915.
Pierani, A., Moran-Rivard, L., Sunshine, M. J., Littman, D. R., Goulding, M. and Jessell, T. M. (2001). Control of interneuron fate in the developing spinal cord by the progenitor homeodomain protein Dbx1. *Neuron* **29**, 367-384.
Polleux, F., Ince-Dunn, G. and Ghosh, A. (2007). Transcriptional regulation of vertebrate axon guidance and synapse formation. *Nat. Rev. Neurosci.* **8**, 331-340.
Prakash, N., Puelles, E., Freude, K., Trümbach, D., Omodei, D., Di Salvio, M., Sussel, L., Ericson, J., Sander, M., Simeone, A. et al. (2009). Nkx6-1 controls the identity and fate of red nucleus and oculomotor neurons in the mouse midbrain. *Development* **136**, 2545-2555.
Saba, R., Nakatsuji, N. and Saito, T. (2003). Mammalian BarH1 confers commissural neuron identity on dorsal cells in the spinal cord. *J. Neurosci.* **23**, 1987-1991.
Sabatier, C., Plump, A. S., Le Ma, Brose, K., Tamada, A., Murakami, F., Lee, E. Y. and Tessier-Lavigne, M. (2004). The divergent Robo family protein rig-1/Robo3 is a negative regulator of slit responsiveness required for midline crossing by commissural axons. *Cell* **117**, 157-169.
Saito, T. (2006). In vivo electroporation in the embryonic mouse central nervous system. *Nat. Protoc.* **1**, 1552-1558.
Schneider, C. A., Rasband, W. S. and Eliceiri, K. W. (2012). NIH Image to ImageJ: 25 years of image analysis. *Nat. Methods* **9**, 671-675.
Shepherd, I. T. and Taylor, J. S. (1995). Early development of efferent projections from the chick tectum. *J. Comp. Neurol.* **354**, 501-510.
Shimogori, T. and Ogawa, M. (2008). Gene application with in utero electroporation in mouse embryonic brain. *Dev. Growth Differ.* **50**, 499-506.
Shirasaki, R. and Pfaff, S. L. (2002). Transcriptional codes and the control of neuronal identity. *Annu. Rev. Neurosci.* **25**, 251-281.
Shirasaki, R., Tamada, A., Katsumata, R. and Murakami, F. (1995). Guidance of cerebellofugal axons in the rat embryo: directed growth toward the floor plate and subsequent elongation along the longitudinal axis. *Neuron* **14**, 961-972.
Shirasaki, R., Mirzayan, C., Tessier-Lavigne, M. and Murakami, F. (1996). Guidance of circumferentially growing axons by netrin-dependent and -independent floor plate chemotropism in the vertebrate brain. *Neuron* **17**, 1079-1088.
Shirasaki, R., Lewcock, J. W., Lettieri, K. and Pfaff, S. L. (2006). FGF as a target-derived chemoattractant for developing motor axons genetically programmed by the LIM code. *Neuron* **50**, 841-853.
Tabata, H. and Nakajima, K. (2001). Efficient in utero gene transfer system to the developing mouse brain using electroporation: visualization of neuronal migration in the developing cortex. *Neuroscience* **103**, 865-872.
Tamada, A., Kumada, T., Zhu, Y., Matsumoto, T., Hatanaka, Y., Muguruma, K., Chen, Z., Tanabe, Y., Torigoe, M., Yamauchi, K. et al. (2008). Crucial roles of Robo proteins in midline crossing of cerebellofugal axons and lack of their up-regulation after midline crossing. *Neural Dev.* **3**, 29.
Tessier-Lavigne, M. and Goodman, C. S. (1996). The molecular biology of axon guidance. *Science* **274**, 1123-1133.
Thaler, J., Harrison, K., Sharma, K., Lettieri, K., Kehrl, J. and Pfaff, S. L. (1999). Active suppression of interneuron programs within developing motor neurons revealed by analysis of homeodomain factor HB9. *Neuron* **23**, 675-687.
Vue, T. Y., Aaker, J., Taniguchi, A., Kazemzadeh, C., Skidmore, J. M., Martin, D. M., Martin, J. F., Treier, M. and Nakagawa, Y. (2007). Characterization of progenitor domains in the developing mouse thalamus. *J. Comp. Neurol.* **505**, 73-91.
Weiner, J. A., Koo, S. J., Nicolas, S., Fraboulet, S., Pfaff, S. L., Pourquié, O. and Sanes, J. R. (2004). Axon fasciculation defects and retinal dysplasias in mice lacking the immunoglobulin superfamily adhesion molecule BEN/ALCAM/SC1. *Mol. Cell. Neurosci.* **27**, 59-69.
Wilson, S. I., Shafer, B., Lee, K. J. and Dodd, J. (2008). A molecular program for contralateral trajectory: Rig-1 control by LIM homeodomain transcription factors. *Neuron* **59**, 413-424.

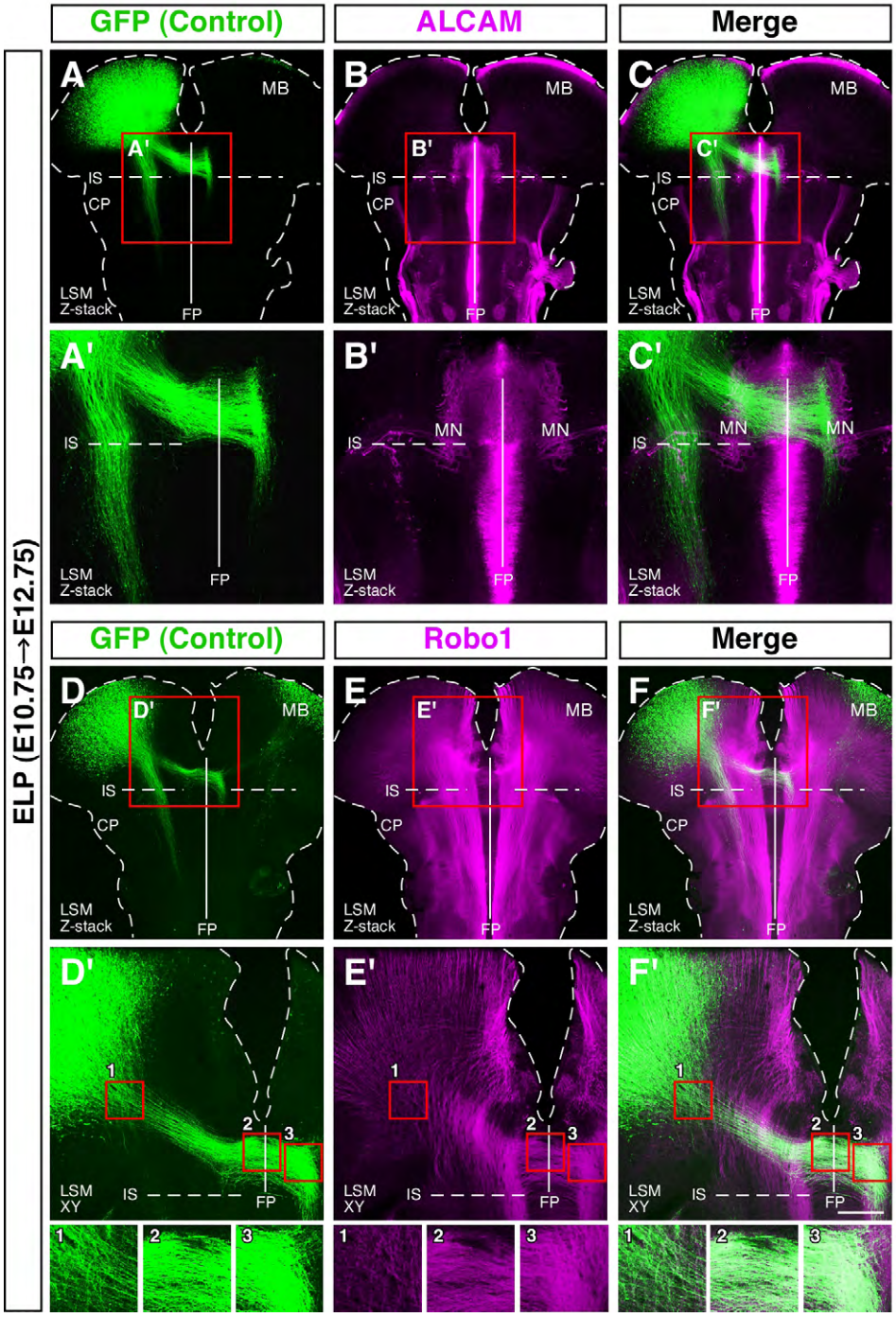

Fig. S1. Trajectory of midbrain commissural axons and the expression pattern of Robo1.

(A-F') GFP-expression vector was electroporated into the dorsal midbrain (MB) at E10.75, and the trajectory of GFP-labeled axons was analyzed in flat-mounted preparations at E12.75, together with immunostaining for expression of ALCAM (B,B') and Robo1 (E,E'). (A-C) Z-stack images of 26 optical sections (10 μm thickness) obtained by confocal LSM. (A'-C') High power views of red rectangles in (A-C), respectively, but showing Z-stack LSM images of 31 optical sections (5 μm thickness). ALCAM staining delineates the location of the floor plate (FP) and oculomotor neurons (MN) in the ventral midbrain. GFP-labeled commissural axons grow caudally in the region between the floor plate and oculomotor neurons on the contralateral side. (D-F) Z-stack images of 25 optical sections (10 μm thickness) obtained by confocal LSM. (D'-F') Higher magnification views of red rectangles in (D-F), respectively, but showing an XY-plane of LSM image. Numbered small red boxes in (D'-F') indicate areas enlarged in corresponding insets below. As midbrain commissural axons grow ventrally toward the floor plate, Robo1 expression on these axons is gradually upregulated. Crossing and post-crossing segments of these commissural axons seem to express higher level of Robo1 compared with the pre-crossing segment. IS, isthmus; CP, cerebellar plate. Scale bar: 600 μm in A-F; 240 μm in A'-F'.

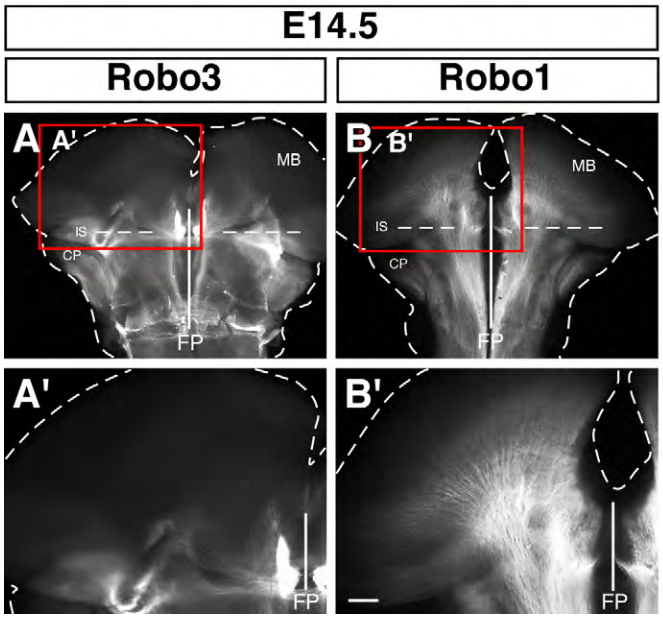

Fig. S2. Expression of Robo3 and Robo1 in the mouse midbrain at E14.5.

(A-B') Immunohistochemical localization of Robo3 and Robo1 in E14.5 flat-mounted preparations. (A,A') Robo3 expression on pre-crossing segment of midbrain commissural axons is downregulated at this stage. (B,B') Expression of Robo1 is still maintained on midbrain ipsilateral axons. (A',B') High power views of red boxes in (A,B), respectively. Scale bar: 500 µm in A,B; 250 µm in A',B'.

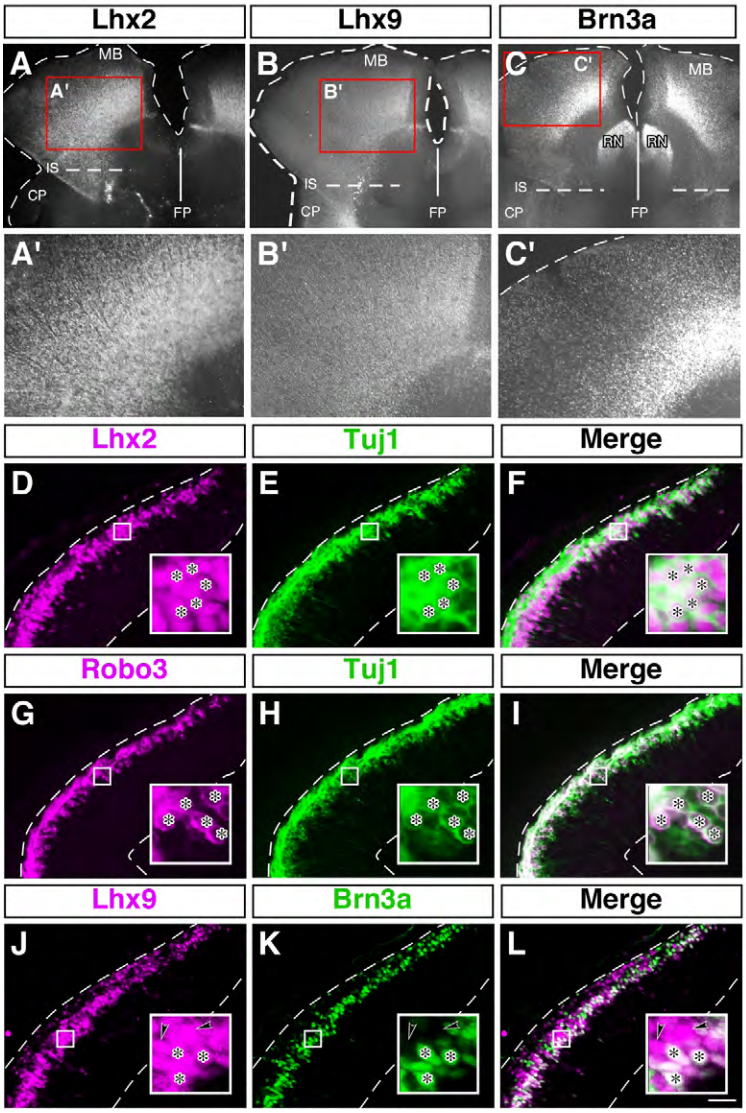

Fig. S3. Expression of transcription factors and Robo3 in the dorsal midbrain.

(A-C') Expression of Lhx2, Lhx9, and Brn3a in flat-mounted preparations at E11.5. (A'-C') High power views of red rectangles in (A-C), respectively. Lhx2 and Lhx9 are selectively expressed in the dorsal midbrain. Brn3a is also expressed in the area where Lhx2 and Lhx9 are expressed. Ventral midbrain cells positive for Brn3a correspond to red nucleus neurons (RN). (D-I) Double-immunostaining analyses for expression of Lhx2/Tuj1 (D-F) and Robo3/Tuj1 (G-I). Lhx2 and Robo3 are expressed by postmitotic neurons, as judged by the expression of Tuj1. Asterisks represent postmitotic neurons expressing Lhx2 and Robo3, respectively (insets). (J-L) Double immunolabeling of Lhx9 and Brn3a in transverse sections of the dorsal midbrain. Similar to the expression of Lhx2 (Fig. 3D-F'), a subset of Lhx9-positive cells expresses Brn3a. Asterisks indicate cells double-positive for Lhx9 and Brn3a, and arrowheads depict Lhx9-positive/Brn3a-negative cells (insets). Small boxes in (D-L) indicate regions enlarged in insets. Scale bar: 250 μm in A-C; 100 μm in A'-C'; 50 μm in D-L.

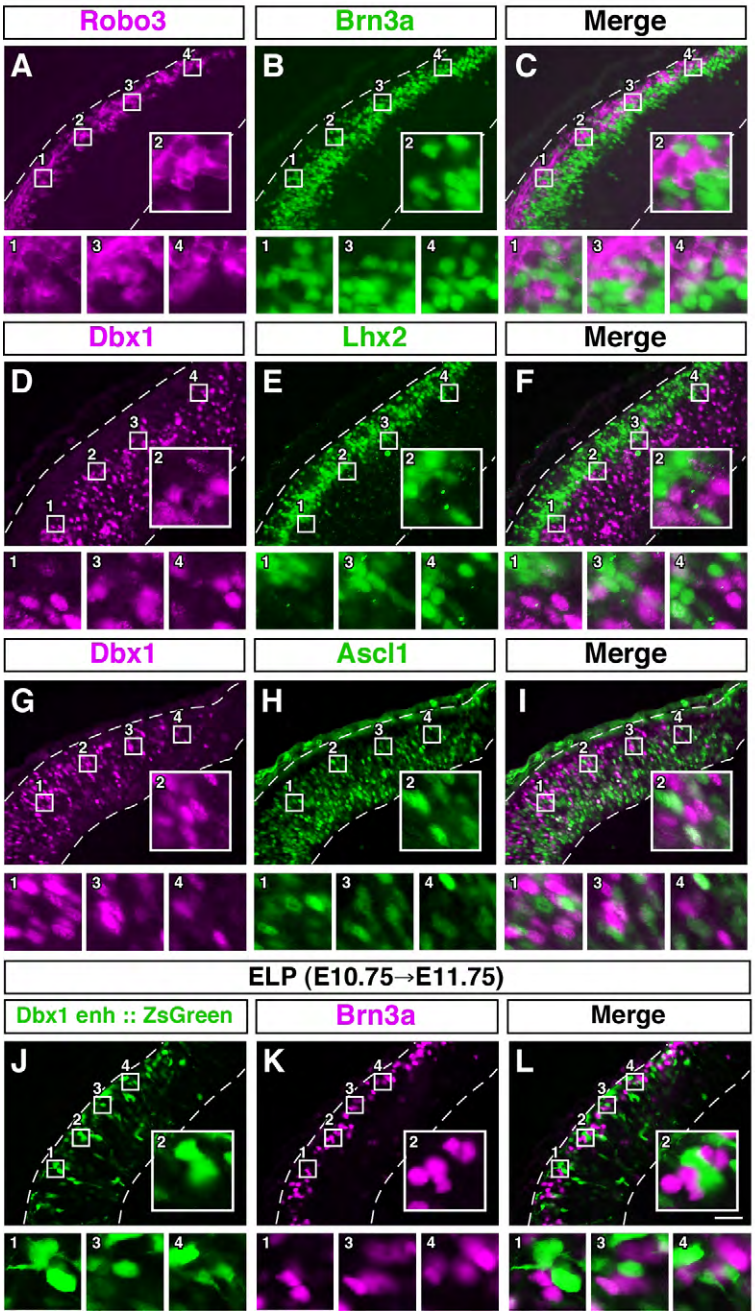

Fig. S4. Detailed expression analyses of transcription factors and Robo3 in the dorsal midbrain.

(A-I) Expression of Brn3a, Dbx1, Lhx2, Ascl1, and Robo3 in transverse cryosections of E11.5 dorsal midbrain. (A-C) Double immunolabeling of Robo3 and Brn3a, showing Robo3-positive cells are segregated from Brn3a-positive cells. (D-F) Dbx1-positive cells do not express Lhx2. (G-I) Dbx1-expressing cells are segregated from Ascl1-positive cells. (J-L) Cell-lineage tracing analyses using *Dbx1*-enhancer element. *In vivo* electroporation of *Dbx1 enhancer::ZsGreen* vector was carried out at E10.75, and the expression of ZsGreen and Brn3a was analyzed in transverse sections at E11.75. ZsGreen-positive cells do not express Brn3a. Numbered small boxes in (A-L) indicate areas enlarged in corresponding insets below. Scale bar: 50 μm.

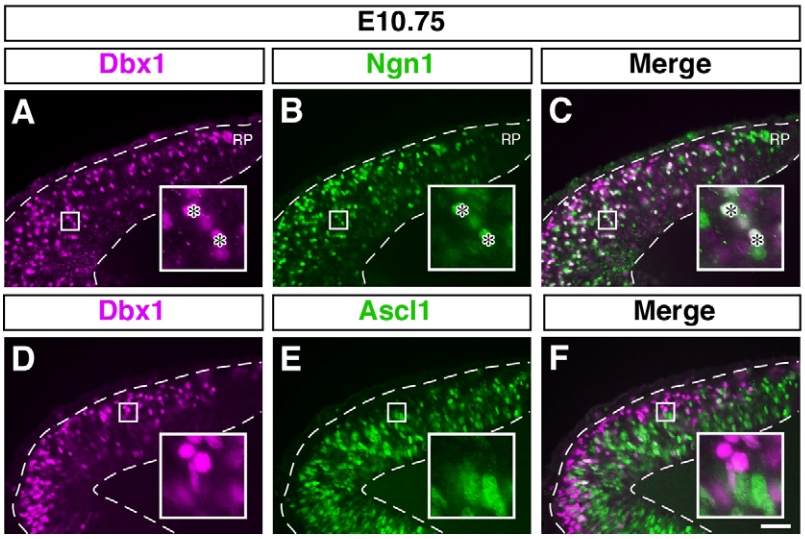

Fig. S5. Expression pattern of Dbx1 in the dorsal midbrain at E10.75.

(A-F) Expression analyses of Dbx1, Ngn1, and Ascl1 in transverse sections of the dorsal midbrain. (A-C) Dbx1 is expressed in subsets of Ngn1-positive progenitors. Asterisks in insets show cells double-positive for Dbx1 and Ngn1. (D-F) Dbx1-positive cells do not express Ascl1. Small boxes in (A-F) indicate areas enlarged in insets. Scale bar: 50 μm. Note that the expression profile and the location of Dbx1-positive cells are basically similar to those observed at E11.5 (Fig. 4). In this study, we show in control embryos that *GFP* plasmids can be successfully targeted into commissural neurons by *in vivo* electroporation at E10.75 compared to E11.5 (Fig.1). Because the overall localization pattern of Dbx1-positive cells is similar between E10.75 and E11.5, it is unlikely that the migration of Dbx1-positive cells away from the ventricle is a direct cause that yields a dramatic difference of the *GFP*-transfection efficiency into commissural neurons. Rather, we reason that, like the case of the relationship between birthdate and laminar fate in the cerebral cortex (Leone et al., 2008, Curr. Opin. Neurobiol. 18, 28-35), a change in the competence of neural stem cells to produce certain progenitor cells committed to express Dbx1 may be involved in the difference of the *GFP*-transfection efficiency.

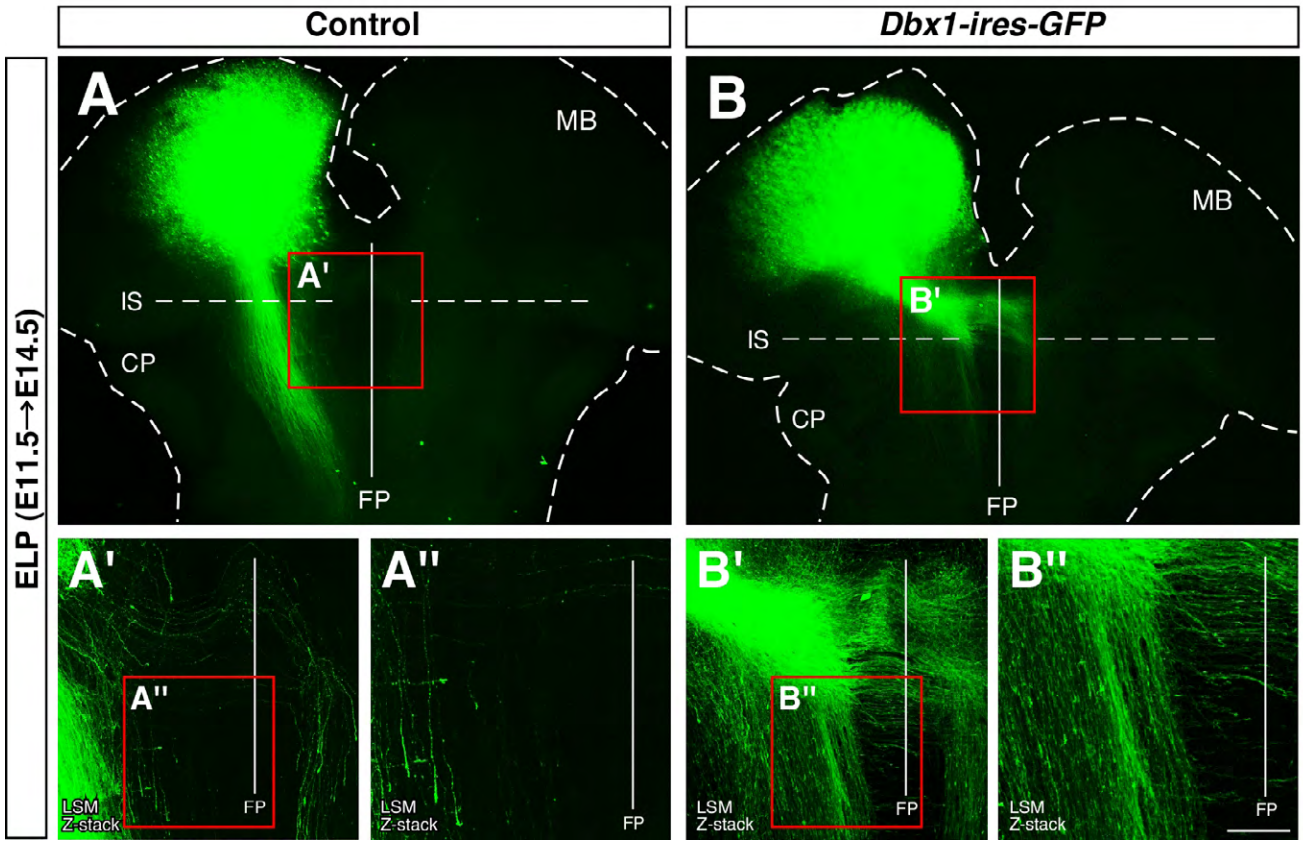

Fig. S6. Change in pathfinding behavior of ipsilateral axons by Dbx1 misexpression.

(A-B") Trajectory of GFP-labeled axons observed in flat-mounted preparations. Electroporation was performed at E11.5, and the axon pathfinding was analyzed at E14.5. (A,A',A") The majority targeted by *GFP* electroporation at this stage are ipsilateral axons (see also Fig. 1C,C'). (A',A") High power views of red rectangle in (A,A'), respectively, but showing a Z-stack image of 35 optical sections (5 µm thickness) obtained by confocal LSM. (A") In controls, ipsilateral axons grow caudally at a distance from the floor plate (FP). (B,B',B") Electroporation of *Dbx1* (*Dbx1-ires-GFP*) at E11.5 causes changes in pathfinding behavior of ipsilateral axons. (B') Pathfinding phenotypes of ipsilateral axons triggered by Dbx1 misexpression. As also shown in Figure 6 (Fig. 6B,B'), midline crossing is dramatically induced. (B") Midline-approaching phenotype represented by a behavior of ipsilateral axons that make a caudal turn at more ventral locations, followed by caudal growth closer to the FP compared with control (A"). (B',B") Higher magnification views of red rectangle in (B, B'), respectively, but showing a Z-stack image of 42 optical sections (5 µm thickness) captured by confocal LSM. Scale bar: 450 µm in A,B; 200 µm in A',B'; 100 µm in A",B".

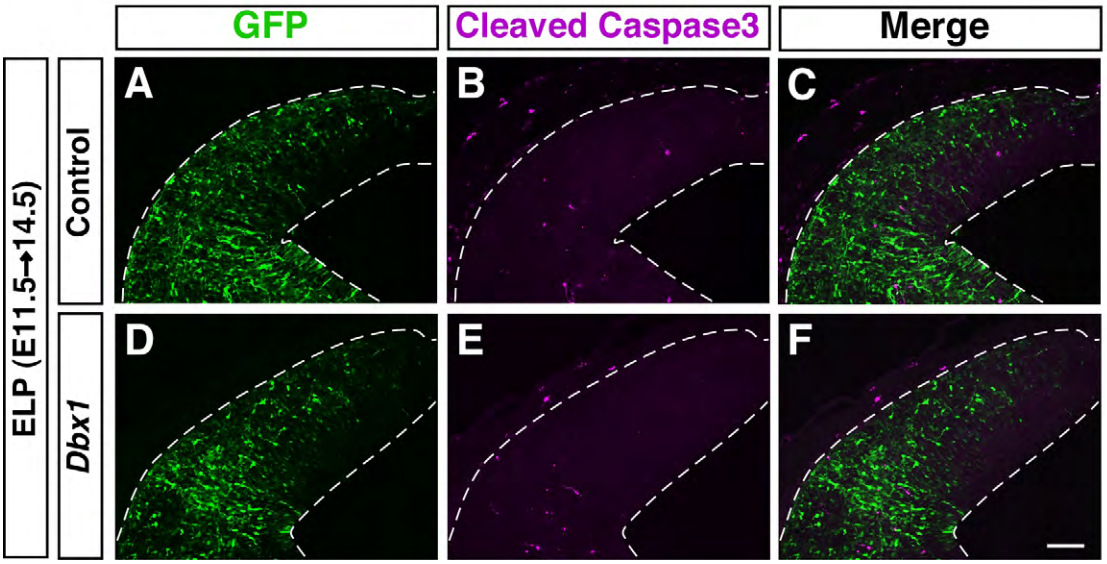

Fig. S7. Cell death analysis in Dbx1-misexpressed dorsal midbrain.

(A-F) Expression of cleaved caspase-3, a marker for detecting apoptotic cells, in the dorsal midbrain of electroporated embryos. Because the number of ipsilateral axons is dramatically reduced in *Dbx1*-electroporated embryos (Fig. 6), we examined whether the decrease in the ipsilateral axons is caused by an apoptotic cell death of ipsilateral neurons due to an effect of *Dbx1* electroporation. (A-C) Expression of cleaved caspase-3 in control embryos (*n*=3). GFP-expression vector was electroporated at E11.5, and immunohistochemistry for expression of cleaved caspase-3 was performed in transverse cryostat sections at E14.5. (D-F) Expression of cleaved caspase-3 in *Dbx1-ires-GFP* electroporated embryos (*n*=4). Note that few apoptotic cells are detected in the midbrain of *Dbx1*-electroporated embryos as well as in controls. Scale bar: 100 μm.

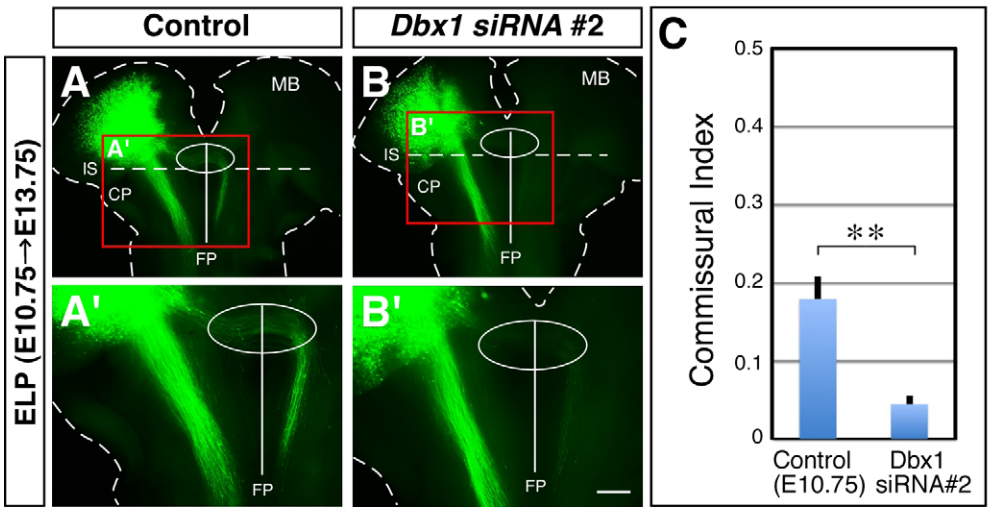

Fig. S8. Phenotype of Dbx1 knockdown using *Dbx1* siRNA (2nd target sequence).

(A,A') Trajectory of GFP-labeled axons in controls. *GFP* electroporation was performed at E10.75, and the electroporated brains were analyzed in flat-mounted preparations at E13.75 (*n*=8). Both commissural and ipsilateral axons are labeled. (B,B') Dbx1 knockdown using *Dbx1* siRNA (2nd target sequence) also results in loss of midline-crossing axons (*n*=7), similarly to that shown in Figure 6 (Fig. 6F,F'). Note that the target sequence used here is different from that employed in Figure 6. (A',B') Higher magnification views of red boxes in (A,B), respectively. (A-B') White oval indicate area around the ventral midbrain tegmentum that includes the floor plate (FP). (C) Quantification of midline crossing evaluated by commissural index (**P<0.01, Mann-Whitney U-test). Error bars indicate s.e.m. Scale bar: 500 μm in A,B; 250 μm in A',B'.

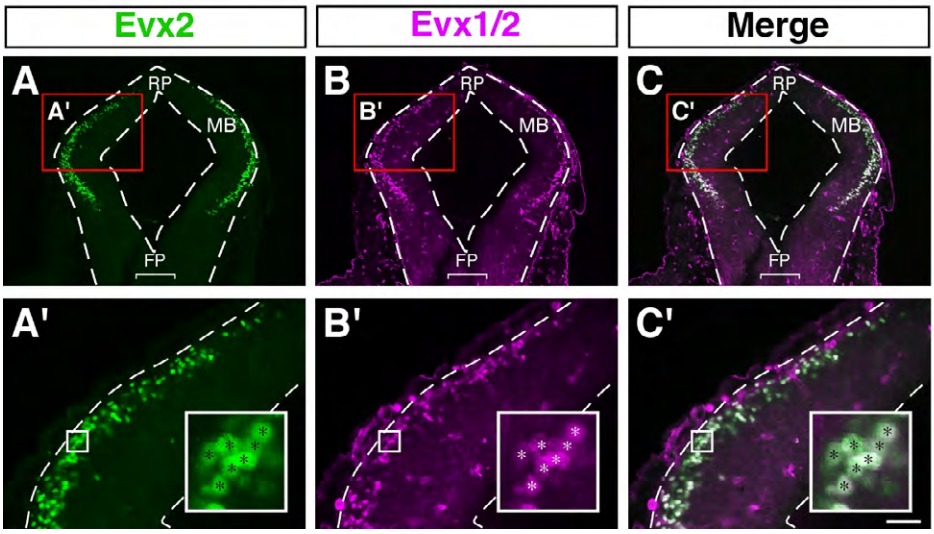

Fig. S9. Expression of Evx2 in the mouse midbrain.

(A-C') Expression of Evx2 in the dorsal midbrain at E11.5. (A'-C') Higher magnification views of red boxes in (A-C), respectively. Small boxes in (A'-C') indicate regions enlarged in insets. Asterisks in insets show that cells immunostained by polyclonal anti-Evx2 correspond precisely to those labeled by a monoclonal anti-Evx1/2 that detects Evx1 and Evx2 (Moran-Rivard et al., 2001, Neuron 29, 385-399; Pierani et al., 2001, Neuron 29, 367-384). Scale bar: 150 μm in A-C; 50 μm in A'-C'.

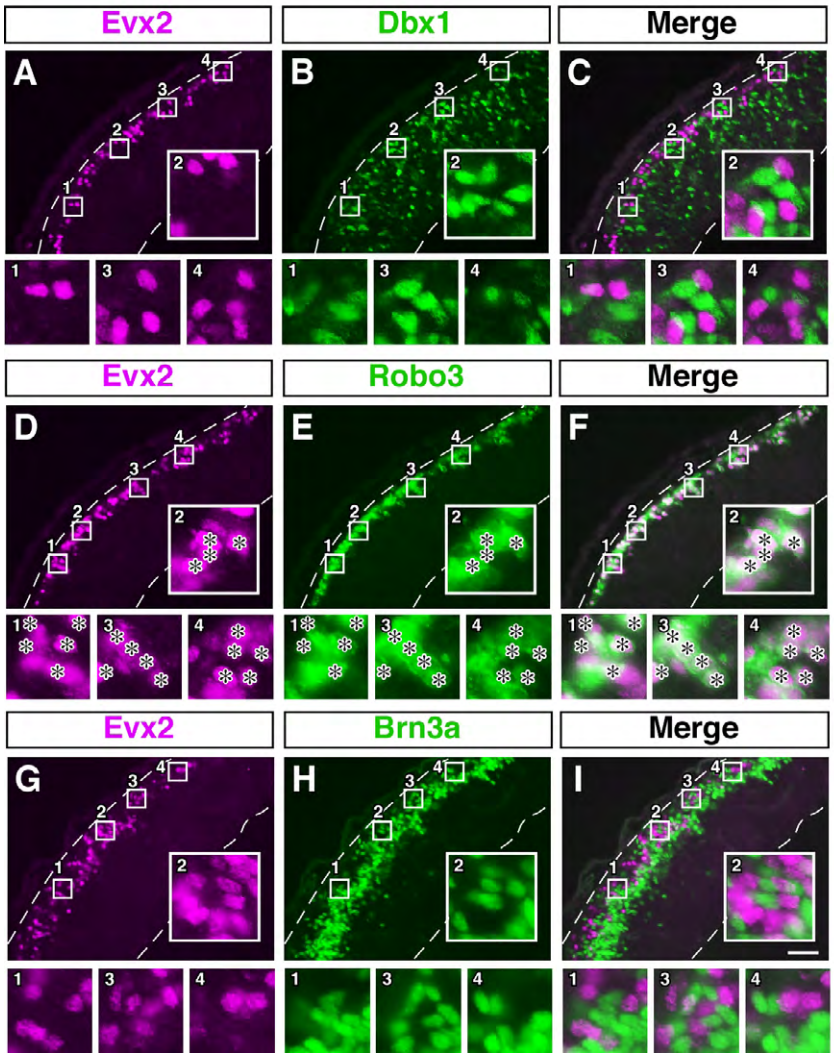

Fig. S10. Detailed expression analyses of Evx2 in the dorsal midbrain.

(A-I) Expression analyses of Evx2 by double-label immunohistochemistry in transverse sections of E11.5 dorsal midbrain. (A-C) Expression of Evx2 does not overlap with that of Dbx1. (D-F) Evx2-expressing cells correspond to Robo3-positive cells. Asterisks represent cells double-positive for Evx2 and Robo3 (insets). Because Robo3 is expressed not only in cell bodies but also on axons, some Robo3-positive/Evx2-negative areas are also observed. (G-I) Co-localization of Evx2 and Brn3a is not observed. Numbered small boxes in (A-I) indicate areas enlarged in corresponding insets below. Scale bar: 50 μm.

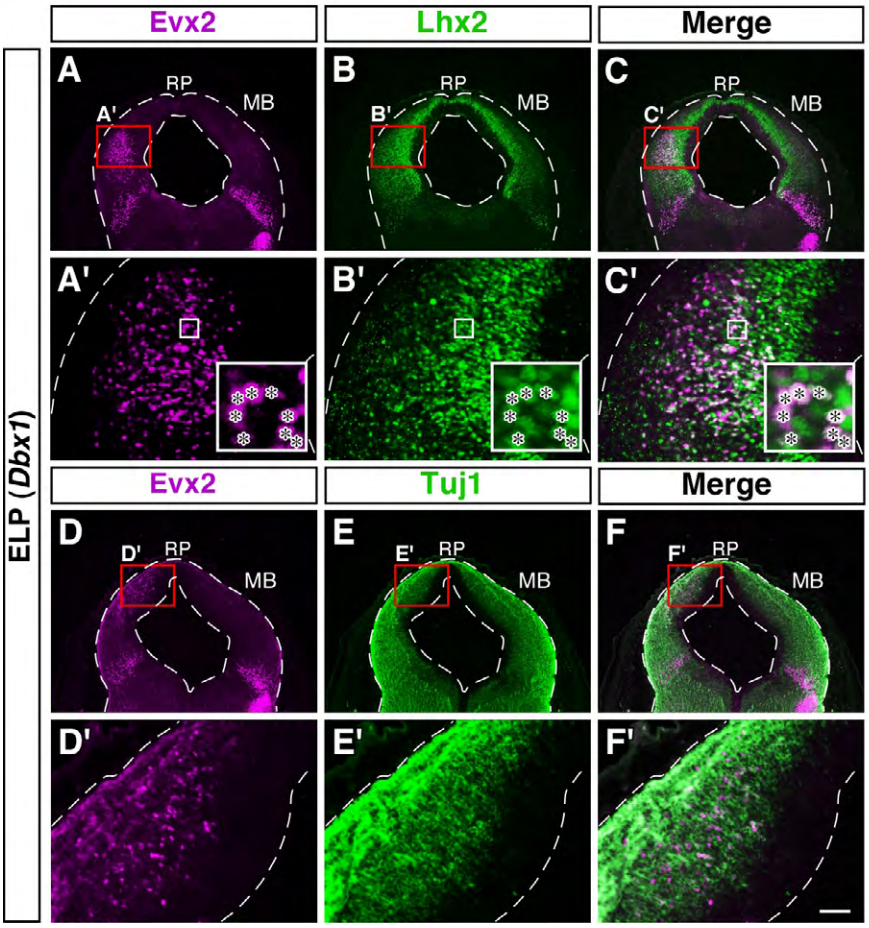

Fig. S11. Expression profile and the location of Evx2-positive cells induced by Dbx1 misexpression.

(A-C') Expression of Lhx2 in Evx2-positive cells that were ectopically induced by Dbx1-misexpression on the left side of the mid-brain. Electroporation of Dbx1-expression vector (without *ires-GFP*) was performed in E11.5 embryos (*n*=4), and the electroporated midbrains were subjected to double-label immunohistochemistry for expression of Evx2 and Lhx2 in transverse sections at E13.5. (A'-C') Higher magnification images of the red boxes in (A-C), respectively. Asterisks represent Evx2-positive cells that express Lhx2 (insets). Small boxes in (A'-C') indicate regions enlarged in insets. (D-F') Evx2-positive cells that were induced by Dbx1-misexpression are located in the postmitotic zone of the dorsal midbrain, as revealed by double immunolabeling of Evx2 and Tuj1 in transverse sections of E13.5 midbrain. Similarly to (A-C'), electroporation of *Dbx1* (without *ires-GFP*) was performed in E11.5 embryos (*n*=4). (D'-F') High power views of red rectangles in (D-F), respectively. Taken together, these results therefore suggest that Evx2-positive cells induced by Dbx1 misexpression undergo similar differentiation program as that operates in normal Evx2-expressing cells in wild type embryos. Scale bar: 250 µm in A-F; 50 µm in A'-F'.

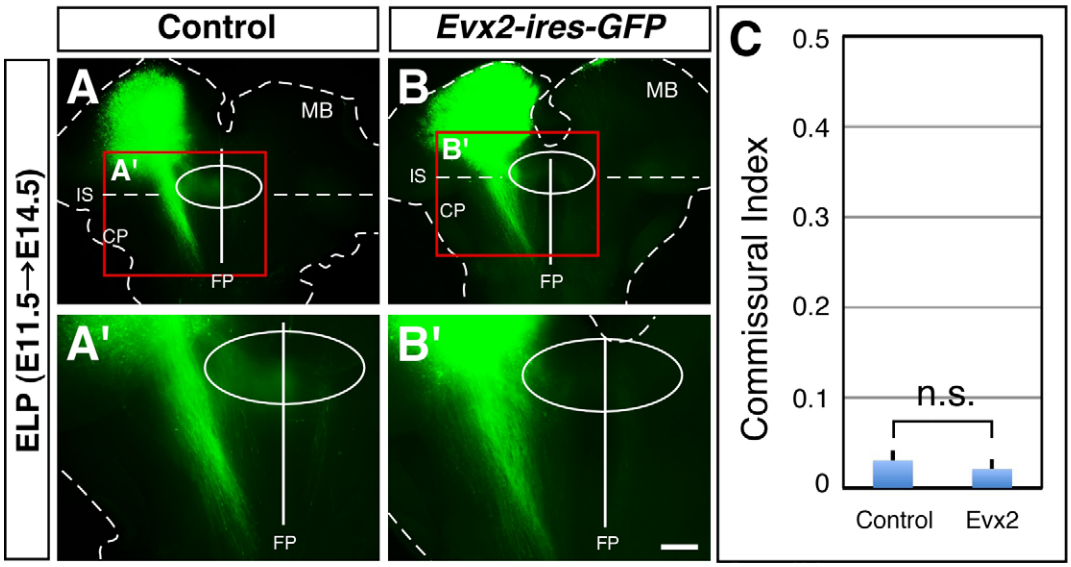

Fig. S12. Effect of Evx2 misexpression on the behavior of ipsilateral axons.

(A,A') Trajectory of GFP-labeled axons in controls. *GFP* electroporation was performed at E11.5, and the axonal trajectory was analyzed in flat-mounted preparations at E14.5 (*n*=10). The majority labeled by GFP are ipsilateral axons. (B,B') Electroporation of *Evx2 (Evx2-ires-GFP)* at E11.5 does not induce midline crossing (*n*=8), contrary to our expectations. We reason that, because Evx2 is a transcription factor normally started to be expressed at the postmitotic stage (Fig. 8), this phenotype may be caused by an atypical cellular context as a result of forced premature expression of Evx2 from the cycling progenitor stage by an electroporation-based gain-of-function approach. Indeed, it has recently been shown that the proper function of Barhl2, a postmitotically-expressed transcription factor that regulates the subtype diversification in the dorsal spinal cord, occurs only when Barhl2 is contextually expressed at the postmitotic stage (Ding et al., 2012, Proc. Natl. Acad. Sci. USA 109, 1566-1571). (A',B') Higher magnification views of red boxes in (A,B), respectively. (A-B') White oval indicate area around the ventral midbrain tegmentum that includes the floor plate (FP). (C) Quantification of midline crossing evaluated by commissural index. Error bars indicate s.e.m. Statistical significance was determined by Mann-Whitney U-test (n.s., not significant). Scale bar: 500 μm in A,B; 250 μm in A',B'.

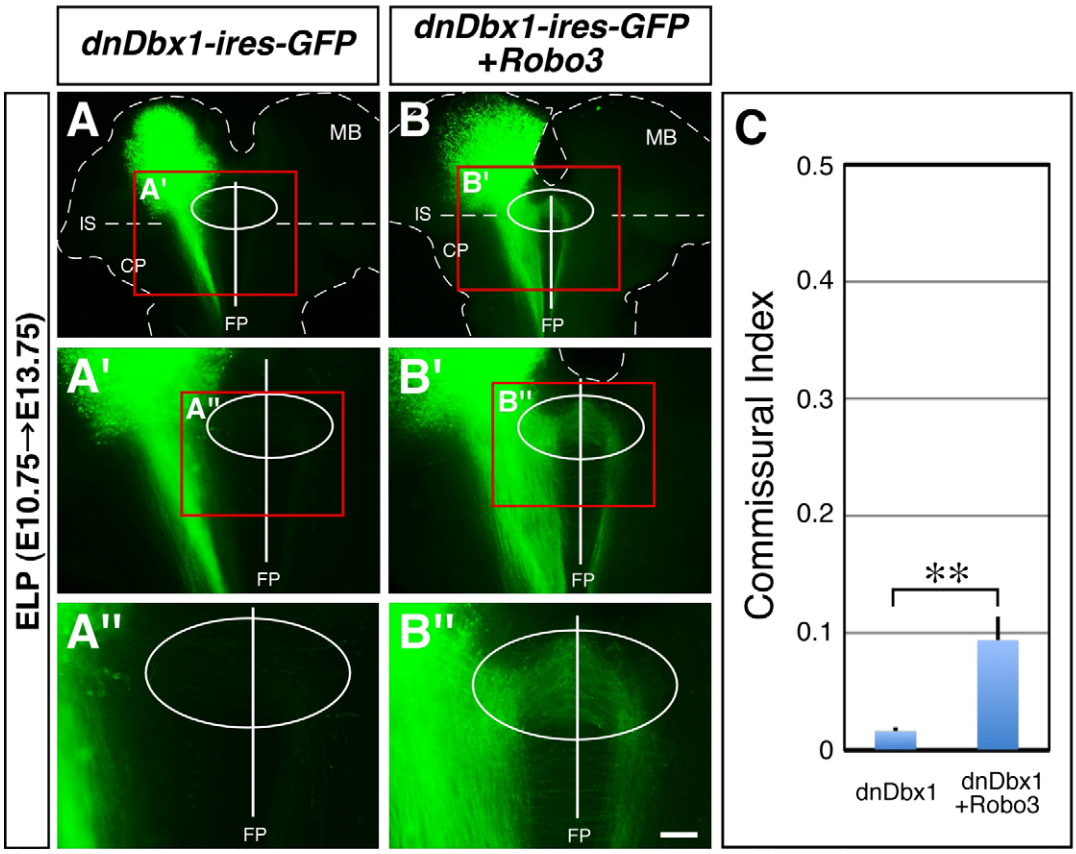

Fig. S13. Restoration of midline-crossing phenotype by Robo3 misexpression in the Dbx1 loss-of-function background.

(A,A',A") Axonal trajectory of *dnDbx1*-electroporated embryos. Electroporation of *dnDbx1* (*dnDbx1-ires-GFP*) was carried out at E10.75, and the effect on midline crossing was analyzed in flat-mounted preparations at 13.75 (*n*=8). Expression of dnDbx1 results in the absence of midline crossing (see also Fig. 6E,E'). (B,B',B") Midline-crossing phenotype is restored by an introduction of *Robo3* in *dnDbx1*-electroporated embryos (*n*=9). (A'-B") Higher magnification views of red rectangles in (A-B'), respectively. (A-G') White oval denotes area around the ventral midbrain tegmentum that includes the floor plate (FP). (C) Quantification of midline crossing evaluated by commissural index. Error bars indicate s.e.m. Statistical significance was determined by Mann-Whitney U-test (**P<0.01). Scale bar: 500 μm in A,B; 250 μm in A',B'; 125 μm in A",B".

Supplemental Table S1. Antibody List

Name	Source	Species	Dilution
Lhx2	Santa Cruz Biotechnology	Goat	1:300
Lhx9	Santa Cruz Biotechnology	Goat	1:100
Brn3a	Millipore	Mouse	1:600
Robo3	R&D Systems	Goat	1:160
Robo3	Tamada et al., 2008	Rabbit	1:500
Robo1	Tamada et al., 2008	Rabbit	1:1000
Tuj1	Covance	Mouse	1:1500
Ki67	BD Pharmingen	Mouse	1:200
Ngn1	Santa Cruz Biotechnology	Goat	1:400
Ascl1	BD Pharmingen	Mouse	1:600
ALCAM	R&D Systems	Goat	1:400
Evx1/2	DSHB	Mouse	1:50
Cleaved Caspase3	Cell Signaling Technology	Rabbit	1:600
GFP	Invitrogen	Rabbit	1:2000
GFP	Invitrogen	Chick	1:2000
ZsGreen1	TaKaRa	Rabbit	1:500